Semi-inclusive deeply inelastic scattering (SIDIS) Theory vs. Data

Wen-Chen Chang

November 12, 2026

References

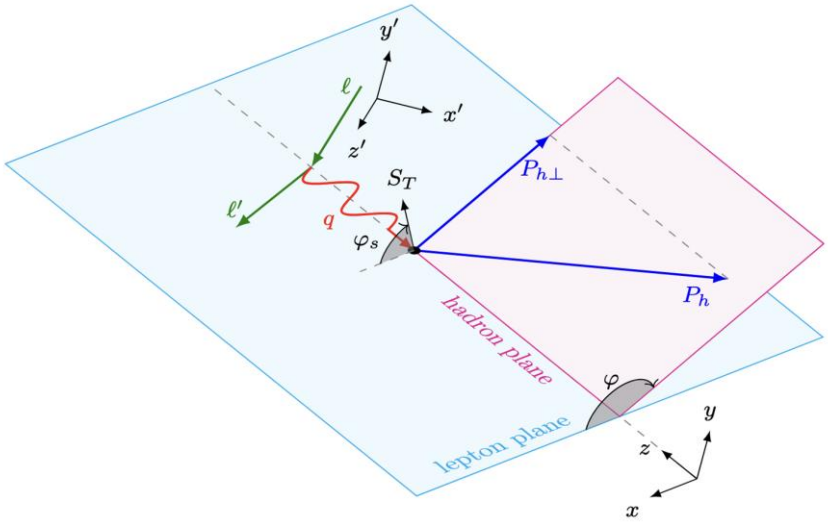
1. SIDIS across transverse momentum Collinear structure and fragmentation at large z
   https://indico.jlab.org/event/1089/contributions/19268/
   https://docs.google.com/presentation/d/1uCfCeNRNYT-Q2H9RRzGXj75hhDThGG3W9H782th2bNI
2. Challenges with Large Transverse Momentum in Semi-Inclusive Deeply Inelastic Scattering
   https://arxiv.org/abs/1808.04396
3. Kinematics of Current Region Fragmentation in Semi-Inclusive Deeply Inelastic Scattering
   https://arxiv.org/abs/1611.10329
4. Mapping the Kinematical Regimes of Semi-Inclusive Deep Inelastic Scattering
   https://arxiv.org/abs/1904.12882
5. New tool for kinematic regime estimation in semi-inclusive deep-inelastic scattering
   https://arxiv.org/abs/2201.12197
6. Current fragmentation in semiinclusive leptoproduction
   https://arxiv.org/abs/hep-ph/0010199
7. Bjorken x weighted energy-energy correlators from the target fragmentation region to the current fragmentation region
   https://arxiv.org/abs/2312.07655

Outline

- SIDIS – variables and frames
- Two issues:
  - Underestimation of yields at pQCD regions
  - Proper identification of current fragmentation
- How EIC could help?
- Summary

Semi-inclusive deeply inelastic scattering (SIDIS)

$$l(l) + \text{Proton}(P) \rightarrow l'(l') + \text{Hadron}(P_H) + X$$



SIDIS is essential for studying the flavor dependence of PDFs and TMDs

$$Q^2 = -q^2 = -(l - l')^2\,, \qquad x_{\rm Bj} = \frac{Q^2}{2P \cdot q}\,,$$

$$x_{\rm N} = -\frac{q^+}{P^+} = \frac{2x_{\rm Bj}}{1 + \sqrt{1 + \frac{4x_{\rm Bj}^2 M^2}{Q^2}}}\,,$$ Nachtmann-x

$$y = \frac{P \cdot q}{P \cdot l}\,, \qquad z_{\rm h} = \frac{P \cdot P_{\rm B}}{P \cdot q} = 2x_{\rm Bj}\frac{P \cdot P_{\rm B}}{Q^2}\,, \qquad z_{\rm N} = \frac{P_{\rm B}^-}{q^-}\,,$$

$$W^2_{\rm tot} = (q + P)^2\,, \qquad W^2_{\rm SIDIS} = (q + P - P_{\rm B})^2\,, \qquad s = (l + P)^2\,.$$

Light-Front Coordinate

Light-cone variables are defined as follows: for a four-vector V^μ,

$$V^\mu = \left(V^+, V^-, \mathbf{V}_{\mathrm{T}}\right) , \tag{A.1}$$

where

$$V^+ = \frac{V^0 + V^z}{\sqrt{2}}, \qquad V^- = \frac{V^0 - V^z}{\sqrt{2}}, \qquad \mathbf{V}_{\mathrm{T}} = \left(V^x, V^y\right) . \tag{A.2}$$

For a four-momentum V, rapidity is defined as usual:

$$y = \frac{1}{2} \ln \left(\left| \frac{V^+}{V^-} \right| \right) . \tag{A.3}$$

In terms of rapidity, light-cone momentum is:

$$V = \left(\frac{M_{\mathrm{T}}}{\sqrt{2}} e^y, \frac{M_{\mathrm{T}}}{\sqrt{2}} e^{-y}, \mathbf{V}_{\mathrm{T}} \right) , \tag{A.4}$$

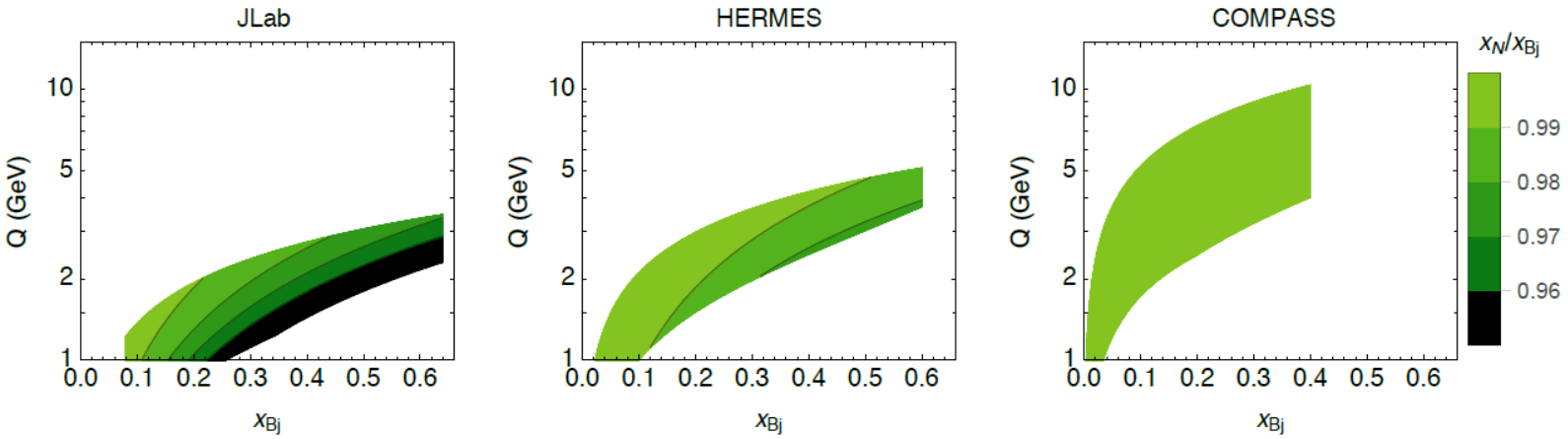
where $V^2 = M^2$ and transverse mass is

$$M_{\mathrm{T}} = \sqrt{\left| M^2 + \mathbf{V}_{\mathrm{T}}^2 \right|} . \tag{A.5}$$

xBj v.s. xN

JHEP10(2019)122

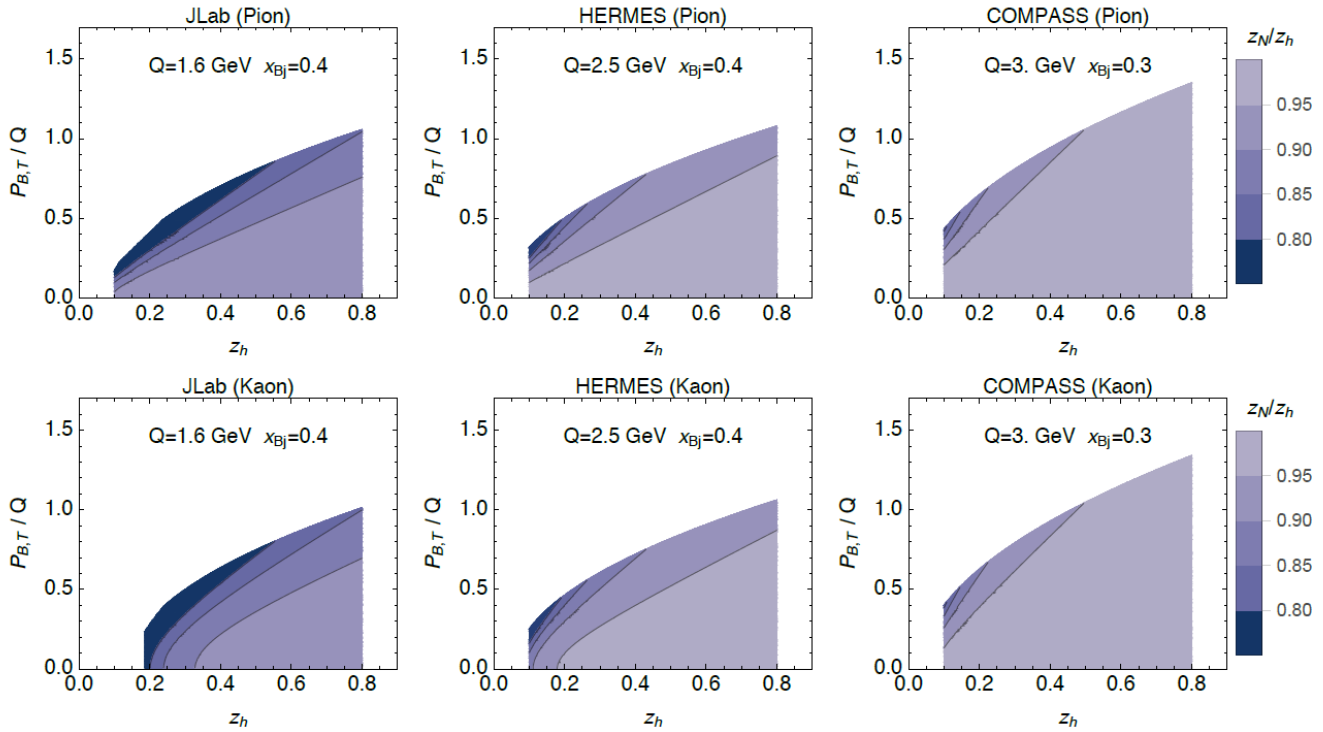
$$x_{\mathrm{N}} = x_{\mathrm{Bj}} \left[1 - \frac{x_{\mathrm{Bj}}^2 M^2}{Q^2} + O\left(\frac{x_{\mathrm{Bj}}^4 M^4}{Q^4} \right) \right]$$



zh v.s. zN

JHEP10(2019)122

$$z_{\mathrm{N}} = z_{\mathrm{h}} \left[1 - \frac{x_{\mathrm{Bj}}^2 M^2}{Q^2} \left(1 + \frac{\mathbf{P}_{\mathrm{B,b,T}}^2}{z_{\mathrm{h}}^2 Q^2} \right) + \left(\frac{x_{\mathrm{Bj}}^2 M^2}{Q^2} \right)^2 \left(\frac{\mathbf{P}_{\mathrm{B,b,T}}^2}{z_{\mathrm{h}}^2 Q^2} - \frac{\mathbf{P}_{\mathrm{B,b,T}}^4}{z_{\mathrm{h}}^4 Q^4} + 2 - \frac{M_{\mathrm{B}}^2}{z_{\mathrm{h}}^2 M^2 x_{\mathrm{Bj}}^2} \right) + O\left(\frac{x_{\mathrm{Bj}}^6 M^6}{Q^6} \right) \right] . \tag{3.2}$$



Photon Frame

JHEP10(2019)122

The virtual photon and the initial proton both have zero transverse momentum, while the final state produced hadron has non-zero transverse momentum:

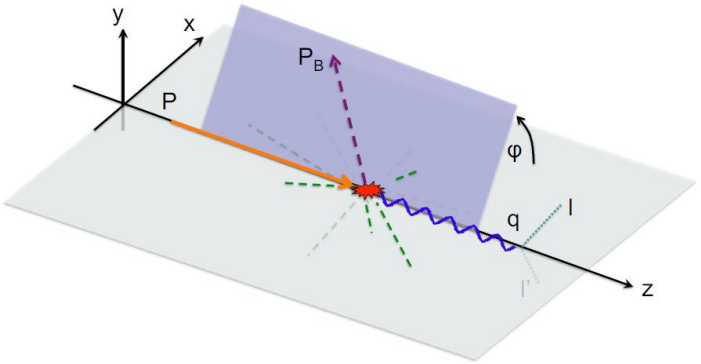


Figure 1. The diagram of a SIDIS event in a photon frame. The hadron plane is shown in purple. The dashed green lines represent unobserved particles.

$$q_\gamma = \left(-x_{\mathrm{N}} P_\gamma^+, \frac{Q^2}{2x_{\mathrm{N}} P_\gamma^+}, \mathbf{0}_{\mathrm{T}}\right),$$

$$P_\gamma = \left(P_\gamma^+, \frac{M^2}{2P_\gamma^+}, \mathbf{0}_{\mathrm{T}}\right),$$

$$P_{\mathrm{B},\gamma} = \left(\frac{\mathbf{P}_{\mathrm{B},\gamma,\mathrm{T}}^2 + M_{\mathrm{B}}^2}{2P_{\mathrm{B},\gamma}^-}, P_{\mathrm{B},\gamma}^-, \mathbf{P}_{\mathrm{B},\gamma,\mathrm{T}}\right).$$

$$P_{\mathrm{H}}^+ = P_\gamma^+ = \frac{Q}{\sqrt{2}x_{\mathrm{N}}}$$

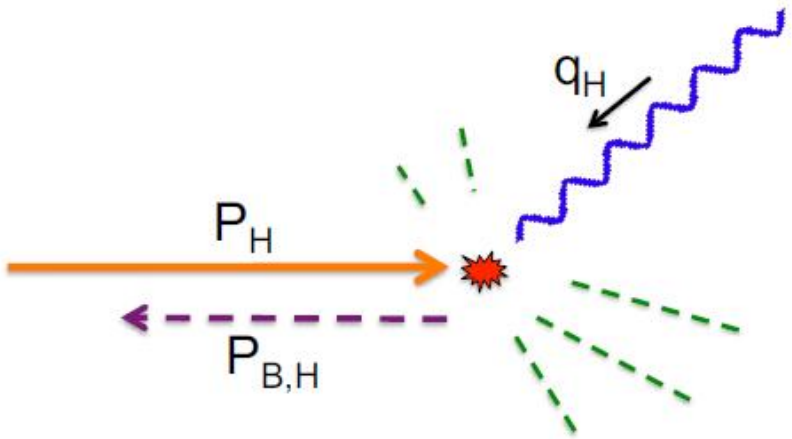
$$P_{\mathrm{H}}^- = P_\gamma^- = \frac{x_{\mathrm{N}} M^2}{\sqrt{2}Q}$$

$$\mathbf{P}_{\mathrm{H,T}} = \mathbf{0}_{\mathrm{T}}.$$

Hadron Frame

JHEP10(2019)122

The incoming hadron and final state hadron are exactly back-to-back (zero relative transverse momentum) while the virtual photon generally has non-zero transverse momentum.



$$q_{\mathrm{H}} = (q_{\mathrm{H}}^{+}, q_{\mathrm{H}}^{-}, \mathbf{q}_{\mathrm{H,T}}) \ ,$$

$$P_{\mathrm{H}} = \left(P_{\mathrm{H}}^{+}, \frac{M^2}{2P_{\mathrm{H}}^{+}}, \mathbf{0}_{\mathrm{T}} \right) \ ,$$

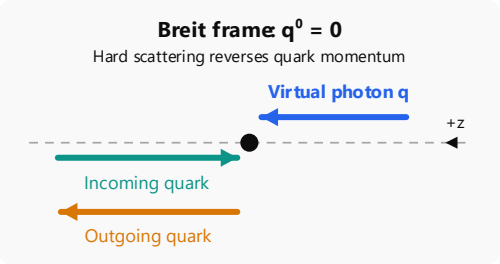
$$P_{\mathrm{B,H}} = \left(\frac{M_{\mathrm{B}}^2}{2P_{\mathrm{B,H}}^{-}}, P_{\mathrm{B,H}}^{-}, \mathbf{0}_{\mathrm{T}} \right) \ .$$

$$P_{\mathrm{H}}^{+} = P_{\gamma}^{+} = \frac{Q}{\sqrt{2}x_{\mathrm{N}}}$$

$$P_{\mathrm{H}}^{-} = P_{\gamma}^{-} = \frac{x_{\mathrm{N}} M^2}{\sqrt{2}Q}$$

$$\mathbf{P}_{\mathrm{H,T}} = \mathbf{0}_{\mathrm{T}} \, .$$

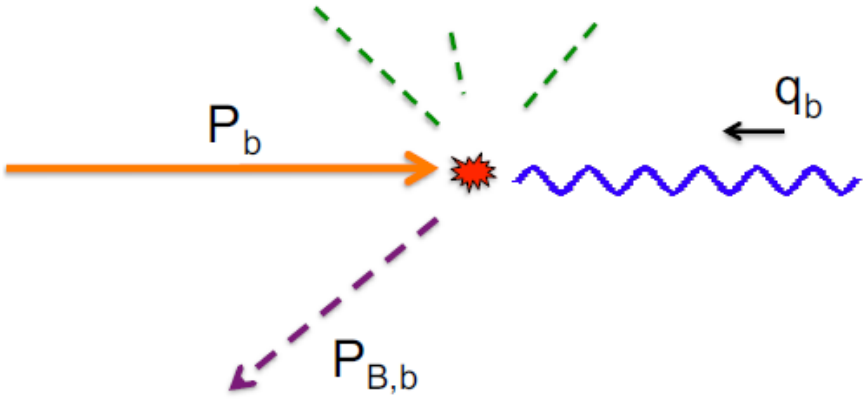
Breit Frame



JHEP10(2019)122

A particular case of the photon frame is the Breit (Brick Wall) frame so that q0 or E =0.
The virtual photon carries purely spatial momentum and zero energy, so the hard scattering can be viewed as reversing the longitudinal momentum of the struck quark.

$$\boxed{q_B^\mu = (0, 0, 0, -Q)}$$



$$q_{\rm b} = \left(-\frac{Q}{\sqrt{2}}, \frac{Q}{\sqrt{2}}, \mathbf{0}_{\rm T}\right),$$

$$P_{\rm b} = \left(\frac{Q}{x_{\rm N}\sqrt{2}}, \frac{x_{\rm N}M^2}{\sqrt{2}Q}, \mathbf{0}_{\rm T}\right) = \left(\frac{M}{\sqrt{2}}\, e^{y_{P,\rm b}}, \frac{M}{\sqrt{2}} e^{-y_{P,\rm b}}, \mathbf{0}_{\rm T}\right).$$

$$P_{\rm B,b} = \left(\frac{M_{\rm B,T}^2}{2P_{\rm B,b}^-}, P_{\rm B,b}^-, \mathbf{P}_{\rm B,b,T}\right) = \left(\frac{M_{\rm B,T}}{\sqrt{2}}\, e^{y_{\rm B,b}}, \frac{M_{\rm B,T}}{\sqrt{2}}\, e^{-y_{\rm B,b}}, \mathbf{P}_{\rm B,b,T}\right)$$

$$P_{\rm B,b} = \left(\frac{M_{\rm B}^2 + z_{\rm N}^2\mathbf{q}_{\rm T}^2}{\sqrt{2}z_{\rm N}Q}, \frac{z_{\rm N}Q}{\sqrt{2}}, -z_{\rm N}\mathbf{q}_{\rm T}\right)$$

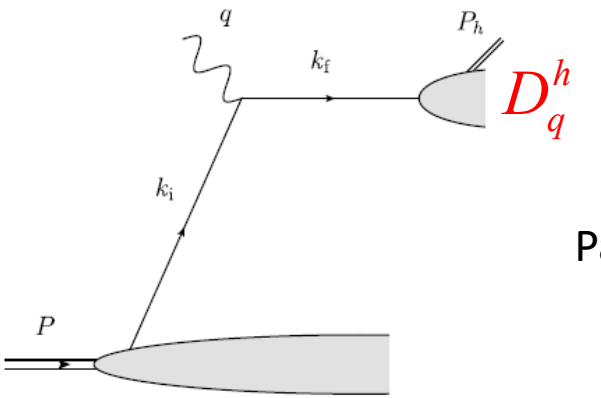
$$M_{\rm B,T} = \sqrt{M_{\rm B}^2 + \mathbf{P}_{\rm B,b,T}^2}$$

$$y_{P,\rm b} \equiv \ln\left(\frac{Q}{x_{\rm N}M}\right), \qquad y_{\rm B,b} \equiv \ln\left(\frac{M_{\rm B,T}}{z_{\rm N}Q}\right)$$

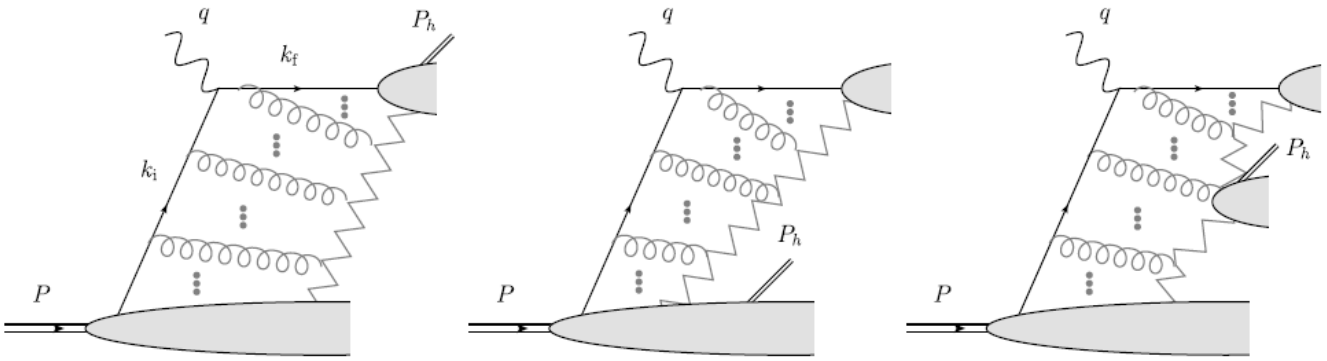
$$\mathbf{q}_{\rm T} \equiv -\frac{\mathbf{P}_{\rm B,b,T}}{z_{\rm N}} = -\frac{q_{\rm b}^-\mathbf{P}_{\rm B,b,T}}{P_{\rm B,b}^-}$$

SIDIS

$$l(l) + \text{Proton}(P) \rightarrow l'(l') + \text{Hadron}(P_H) + X$$



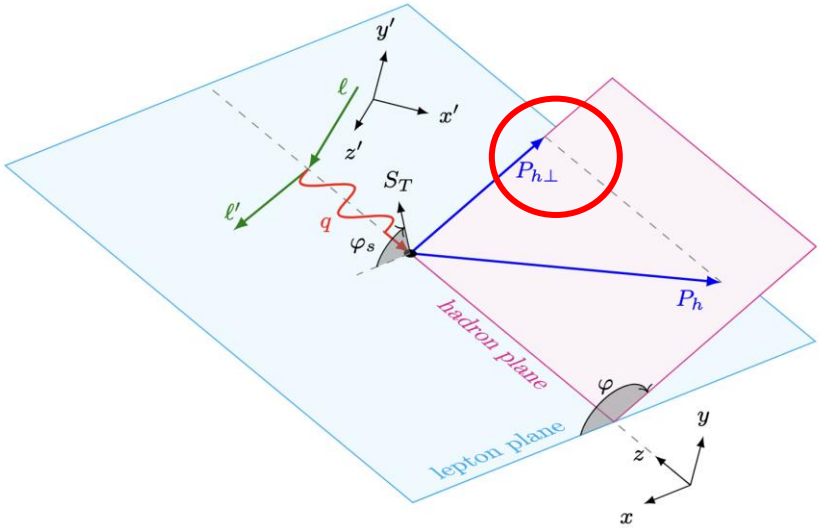
Parton model



(a) (b) (c)

Current fragmentation Target fragmentation Central region

Small and large transverse momentum

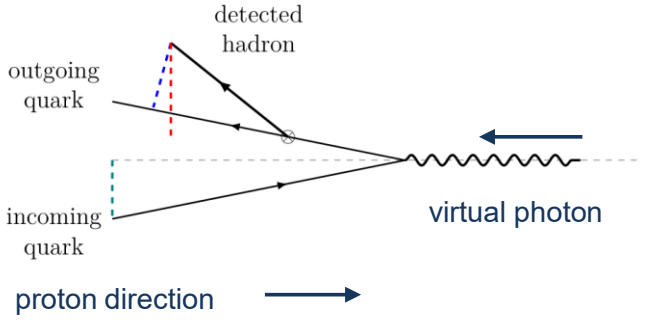


The same measured spectrum contains different mechanisms.

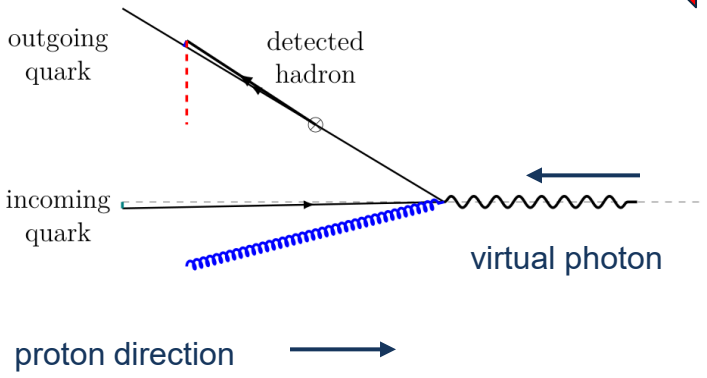
$q_T \simeq P_{hT}/z_h$

This quantity that appears as a second scale enables to define what is small and what large relative to Q

$q_T \ll Q$: TMD factorization

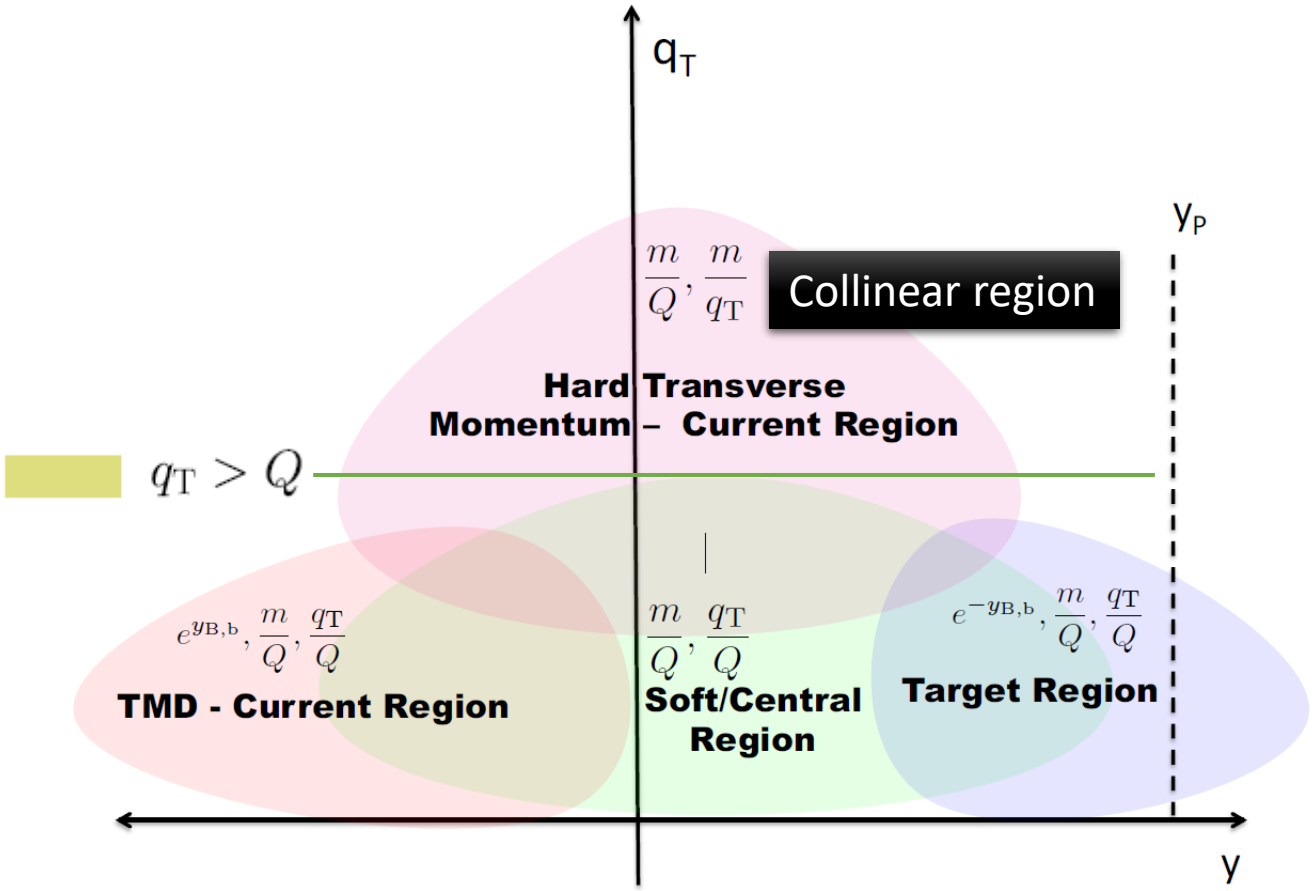


$q_T \sim Q$: collinear factorization



Kinematical regions of SIDIS

JHEP10(2019)122



Fragmentation Functions D(z, Q2)

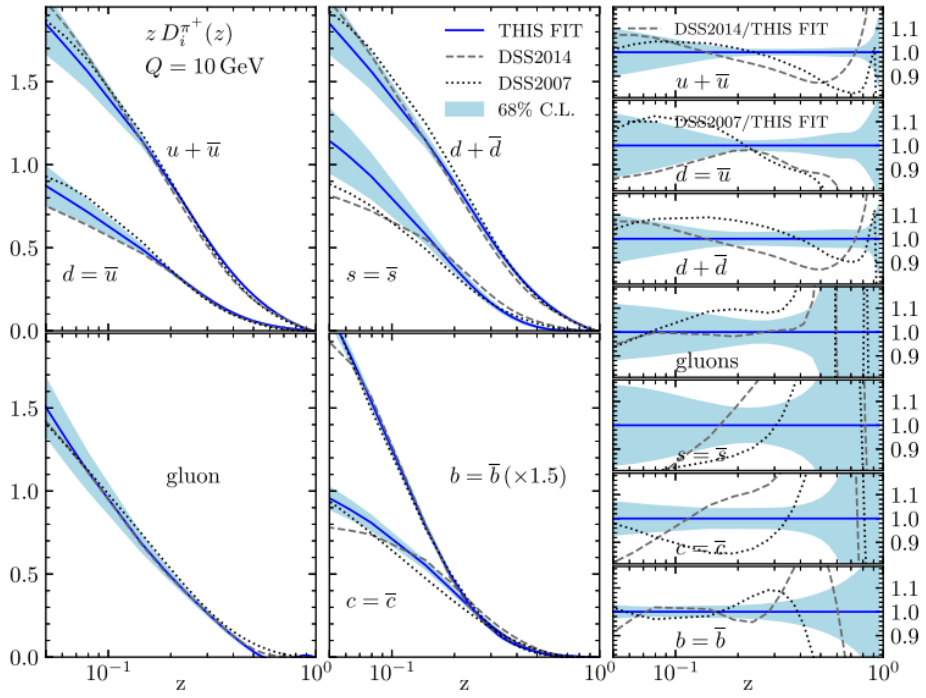
https://journals.aps.org/prd/pdf/10.1103/PhysRevD.75.114010
https://journals.aps.org/prd/pdf/10.1103/PhysRevD.105.L031502

$$\frac{d\sigma^H}{dxdydz_H} = \frac{2\pi\alpha^2}{Q^2}\left[\frac{(1+(1-y)^2)}{y} 2F_1^H(x, z_H, Q^2) + \frac{2(1-y)}{y} F_L^H(x, z_H, Q^2)\right],$$

$$2F_1^H(x, z_H, Q^2) = \sum_{q,\bar{q}} e_q^2 \left\{ q(x, Q^2) D_q^H(z_H, Q^2) + \frac{\alpha_s(Q^2)}{2\pi}[q \otimes C_{qq}^1 \otimes D_q^H + q \otimes C_{gq}^1 \otimes D_g^H + g \otimes C_{qg}^1 \otimes D_q^H] \times (x, z_H, Q^2) \right\},$$

$$F_L^H(x, z_H, Q^2) = \frac{\alpha_s(Q^2)}{2\pi} \sum_{q,\bar{q}} e_q^2 [q \otimes C_{qq}^L \otimes D_q^H + q \otimes C_{gq}^L \otimes D_g^H + g \otimes C_{qg}^L \otimes D_q^H] \times (x, z_H, Q^2),$$

$z_H > 0.2$: the current fragmentation



$z_H \equiv p_H \cdot p_N / p_N \cdot q$

TABLE I. Data sets, normalizations N_i as defined in Eq. (6) of [8], and the partial and total χ^2 values obtained in the fit.

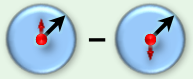
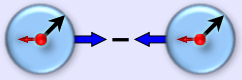
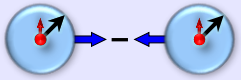
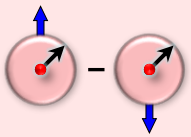
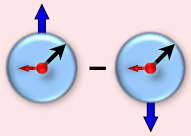
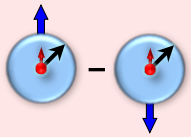
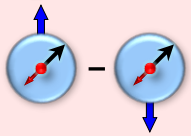
Experiment		Data type	N_i	Number of data in fit	χ^2
TPC [35]	29 GeV	inclusive	1.038	17	22.0
		uds, c, b tag	1.038	27	16.6
TASSO [36]	34 GeV	inclusive	1.038	11	28.4
	44 GeV	inclusive	1.038	7	20.8
SLD [37]	91.2 GeV	inclusive	0.977	28	19.5
		uds, c, b tag	0.977	51	39.2
ALEPH [38]	91.2 GeV	inclusive	1.012	22	44.5
DELPHI [39]	91.2 GeV	inclusive	1.000	17	23.0
		uds, b tag	1.000	34	33.8
OPAL [40]	91.2 GeV	inclusive	1.000	21	31.5
		u, d, s, c, b tag	0.793	25	62.1
BABAR [10]	10.54 GeV	inclusive	1.060	45	142.4
BELLE [9]	10.52 GeV	inclusive	1.067	78	60.2
SIA data (sum)				378	544.1
HERMES [33]	π^+,π^-	(p-Q^2)	0.984	56	54.3
	π^+,π^-	(d-Q^2)	0.988	56	46.5
	π^+,π^-	(p-x)	1.007	56	159.5
	π^+,π^-	(d-x)	1.009	56	189.5
COMPASS [11]	π^+,π^-	(d-z)	1.004	510	302.1
SIDIS data (sum)				734	751.9
BRAHMS [41]	0.20 TeV	π^+,π^-	1.313	26	13.5
STAR [16–19]	0.20 TeV	π^0	1.190	12	8.2
	0.20 TeV	π^0	0.921	7	4.0
	0.20 TeV	π^+,π^-	1.029	26	37.3
	0.20 TeV	π^+,π^-	1.158	34	73.8
PHENIX [20,21]	0.20 TeV	π^0	1.177	22	13.8
	0.51 TeV	π^0	1.178	27	32.9
ALICE [12–15]	0.90 TeV	π^0	1.012	7	52.0
	2.76 TeV	π^0	1.002	24	17.4
	2.76 TeV	$\pi^\pm$	0.959	38	15.6
	7 TeV	π^0	1.016	25	30.6
	7 TeV	$\pi^\pm$	0.976	32	23.9
	8 TeV	π^0,	1.048	36	34.5
	13 TeV	$\pi^\pm$	0.981	32	56.2
PP data (sum)				348	413.7
TOTAL:				1460	1709.7

Leading-Twist Transverse-momentum Dependent **Parton Density Function** (TMDs)

spin of the nucleon

spin of the parton

k_T of the parton

Nucleon \ Quark, Gluon	U	L	T
U	number density $f_1^{q,g}(x,k_T^2)$		 Boer-Mulders $h_1^{\perp q,g}(x,k_T^2)$
L		 Helicity $g_{1L}^{q,g}(x,k_T^2)$	 worm-gear L $h_{1L}^{\perp q,g}(x,k_T^2)$
T	 Sivers $f_{1T}^{\perp q,g}(x,k_T^2)$	 Kotzinian-Mulders worm-gear T $g_{1T}^{\perp q,g}(x,k_T^2)$	 Transversity $h_1^{q,g}(x,k_T^2)$  Pretzelosity $h_{1T}^{\perp q,g}(x,k_T^2)$

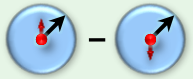
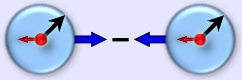
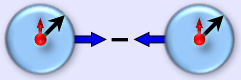
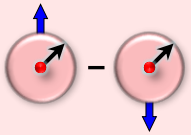
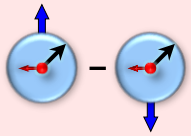
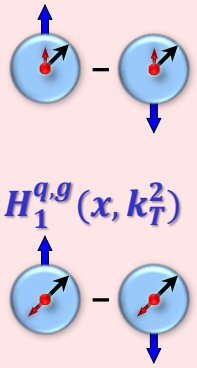
	T-even	T-odd
chiral-even	$f_1,\ g_{1L},\ g_{1T}$	$f_{1T}^{\perp}$
chiral-odd	$h_1,\ h_{1L}^{\perp},\ h_{1T}^{\perp}$	$h_1^{\perp}$

Leading-Twist Transverse-momentum Dependent **Fragmentation Function** (TMDs)

spin of the nucleon

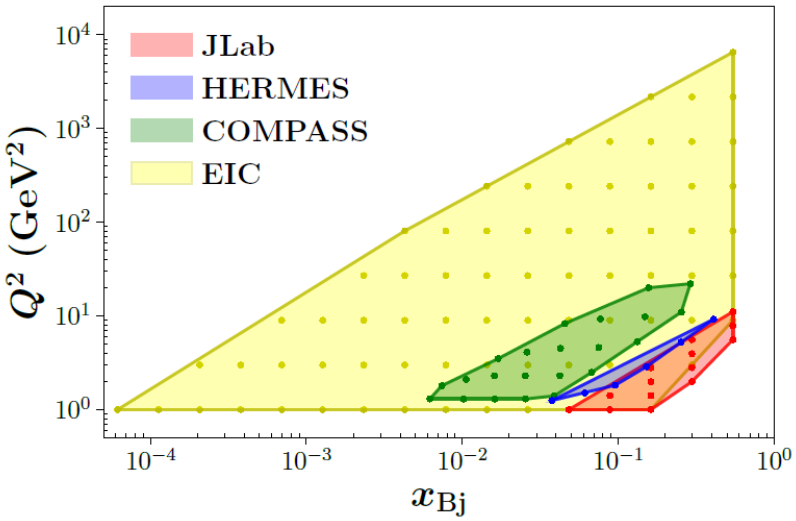
spin of the parton

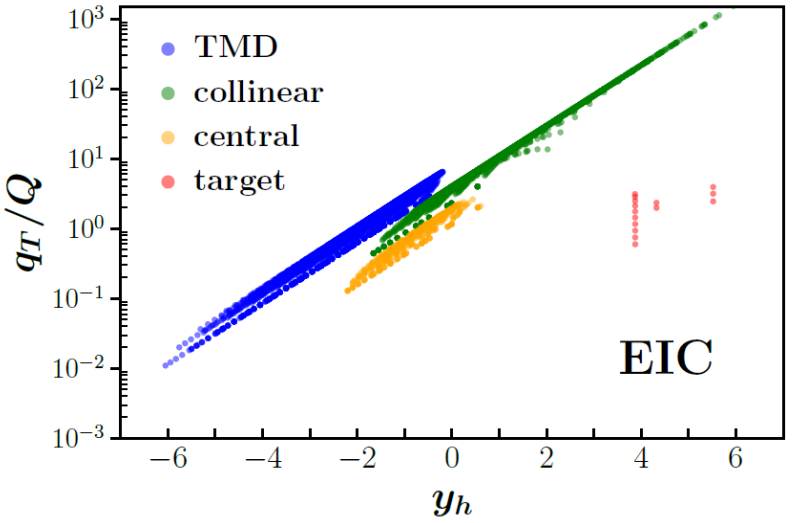
k_T of the parton

Nucleon \ Quark, Gluon	U	L	T
U	 unpolarized $D_1^{q,g}(x,k_T^2)$		 Collins $H_1^{\perp q,g}(x,k_T^2)$
L		 $G_{1L}^{q,g}(x,k_T^2)$	 $H_{1L}^{\perp q,g}(x,k_T^2)$
T	 $D_{1T}^{\perp q,g}(x,k_T^2)$	 $G_{1T}^{\perp q,g}(x,k_T^2)$	 $H_1^{q,g}(x,k_T^2)$ $H_{1T}^{\perp q,g}(x,k_T^2)$

	T-even	T-odd
chiral-even	$D_1,\ G_{1L},\ G_{1T}$	$D_{1T}^{\perp}$
chiral-odd	$H_1,\ H_{1L}^{\perp},\ H_{1T}^{\perp}$	$H_1^{\perp}$

Fixed-Target vs. EIC (H1)





Fixed-order pQCD calculations and SIDIS measurements (H1)

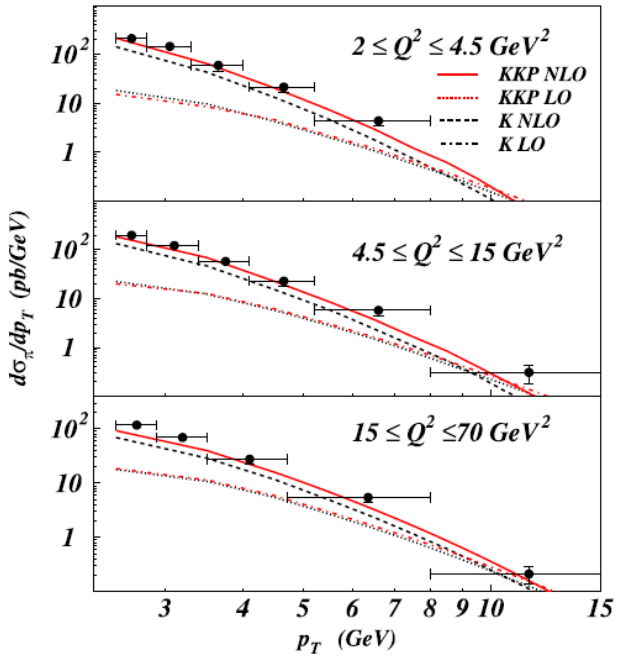
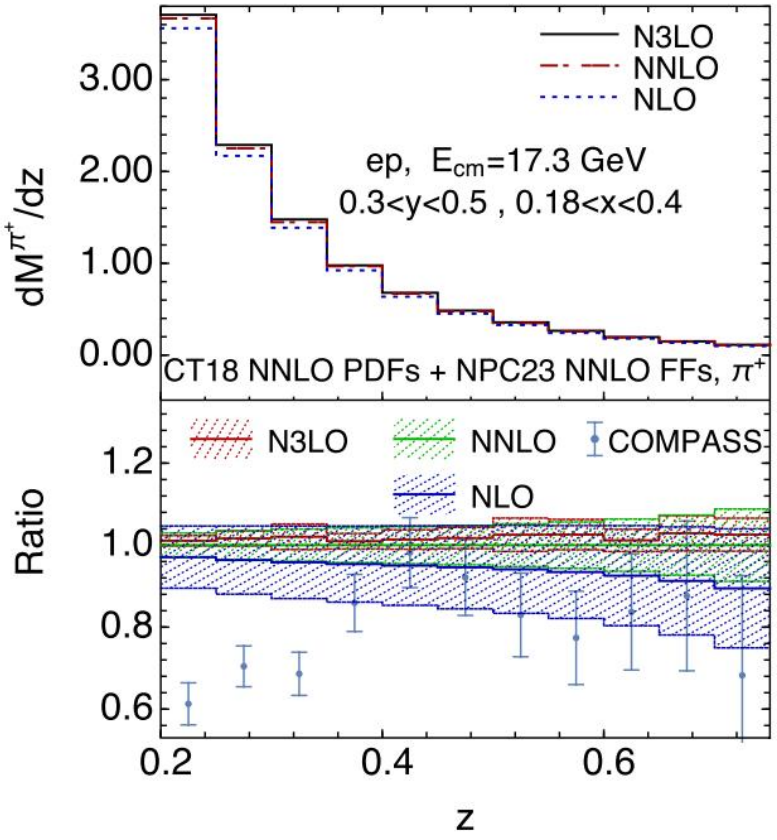


FIG. 3. Figure 4 from Ref. [24]. The differential cross section was integrated over x, z, and bins of Q with H1 cuts, calculated with both leading order and next-to-leading order, and compared with π^0 production data from Ref. [23]. Here, p_T corresponds to our $P_{H,\mathrm{T}}$; see Eq. (1). Note the large correction from $O(\alpha_s^2)$.

Fixed-order pQCD calculations and SIDIS measurements (COMPASS)

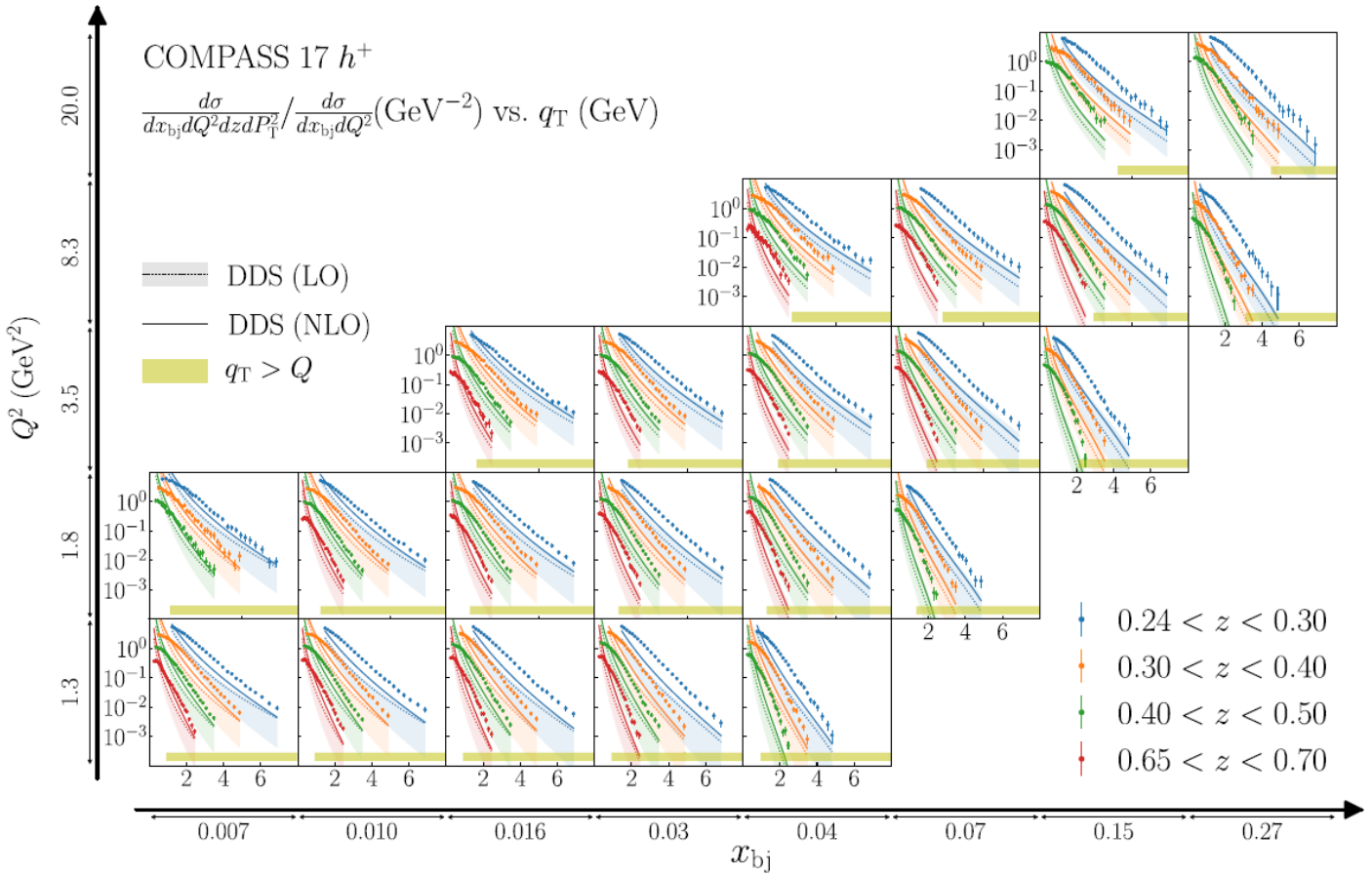
PRL 137, 151901 (2026)



Theoretical predictions overshoot the data

Fixed-order pQCD calculations and SIDIS measurements (COMPASS)

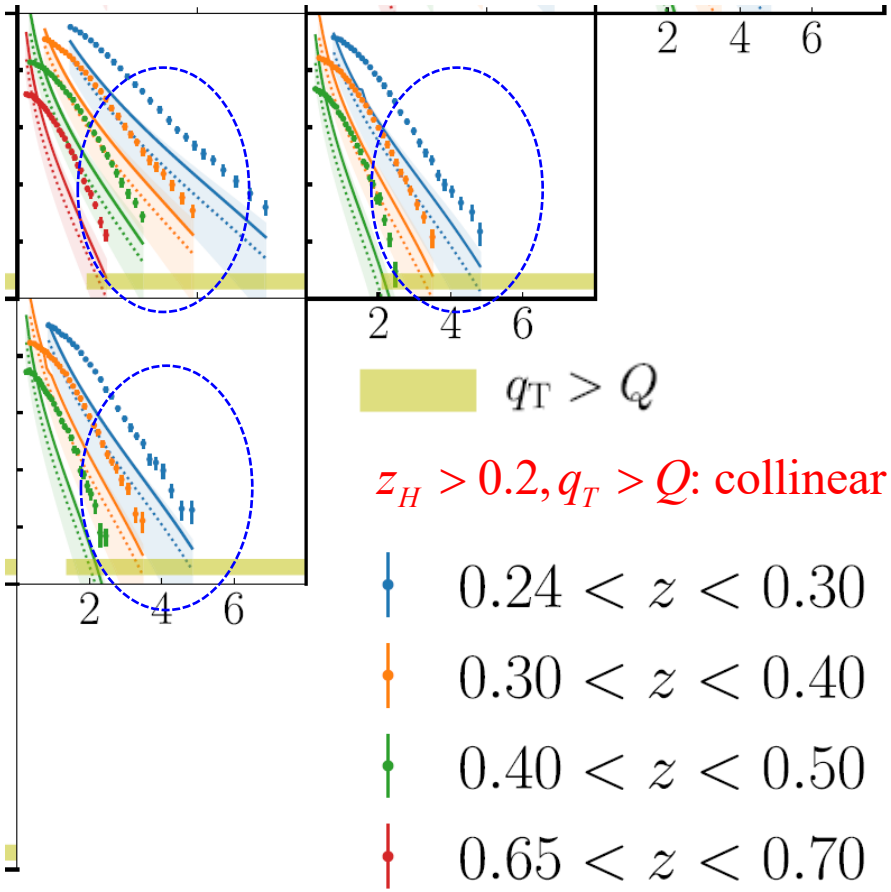
PRD 98, 114005 (2018)



Theoretical predictions underestimate the data at large-qT (pQCD/collinear) regions.

Fixed-order pQCD calculations and SIDIS measurements (COMPASS)

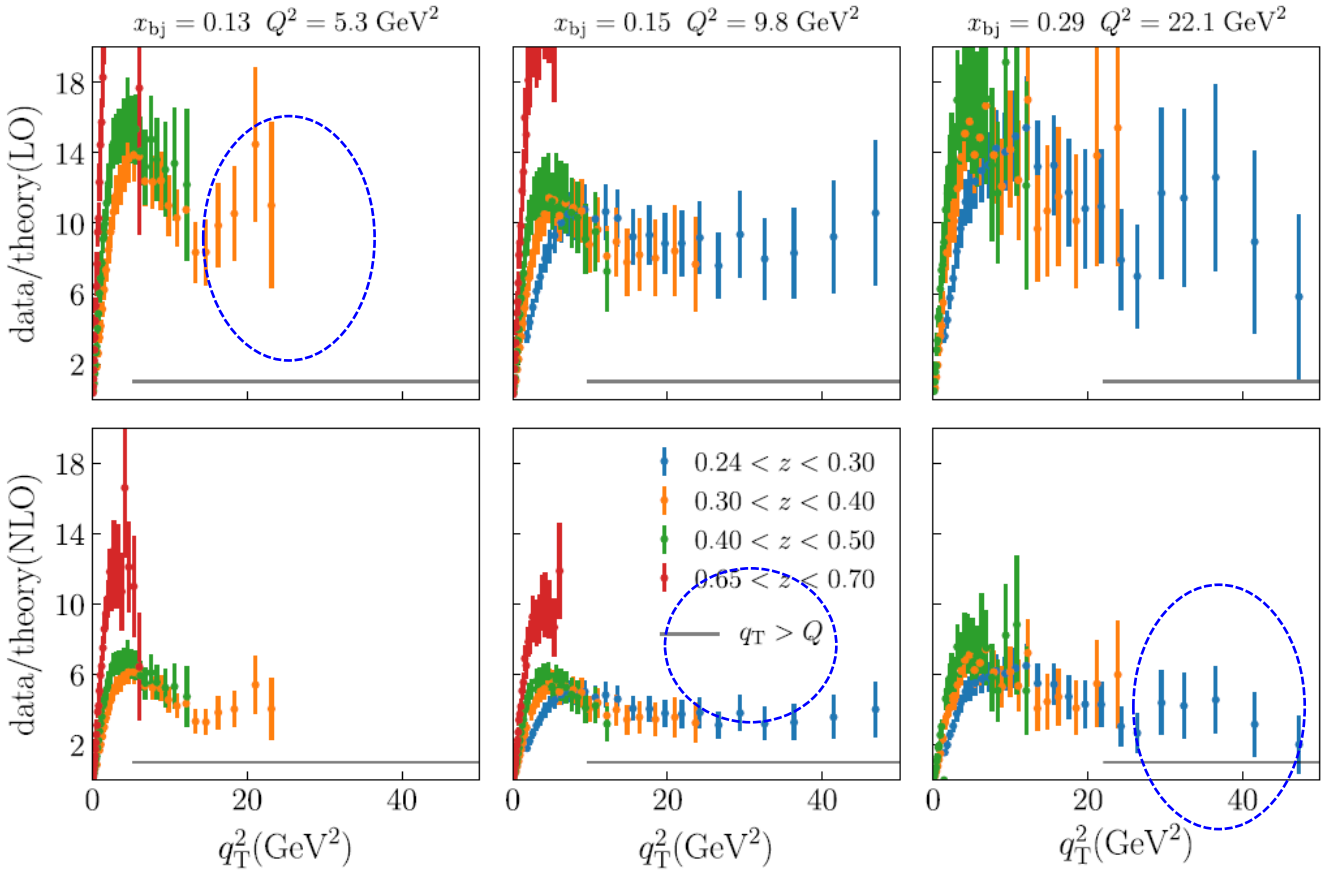
PRD 98, 114005 (2018)



Theoretical predictions underestimate the data at large-qT (pQCD/collinear) regions.

Ratio of data to theory (COMPASS)

PRD 98, 114005 (2018)



$z_H > 0.2, q_T > Q$: collinear current fragmentation

Theoretical predictions underestimate the data at large-qT (pQCD/collinear) regions.

Fixed-order pQCD calculations and SIDIS measurements (HERMES)

PRD 98, 114005 (2018)

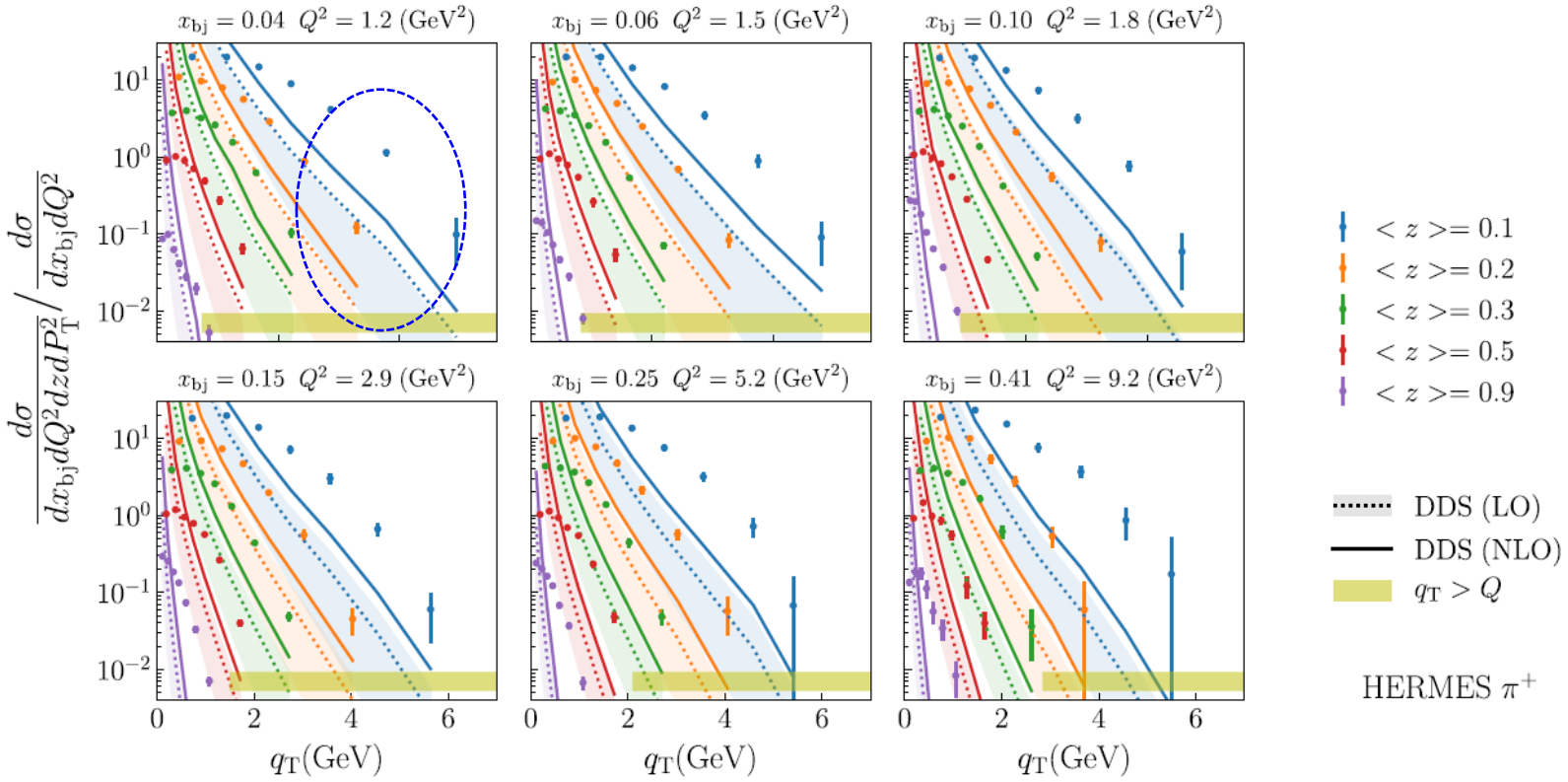
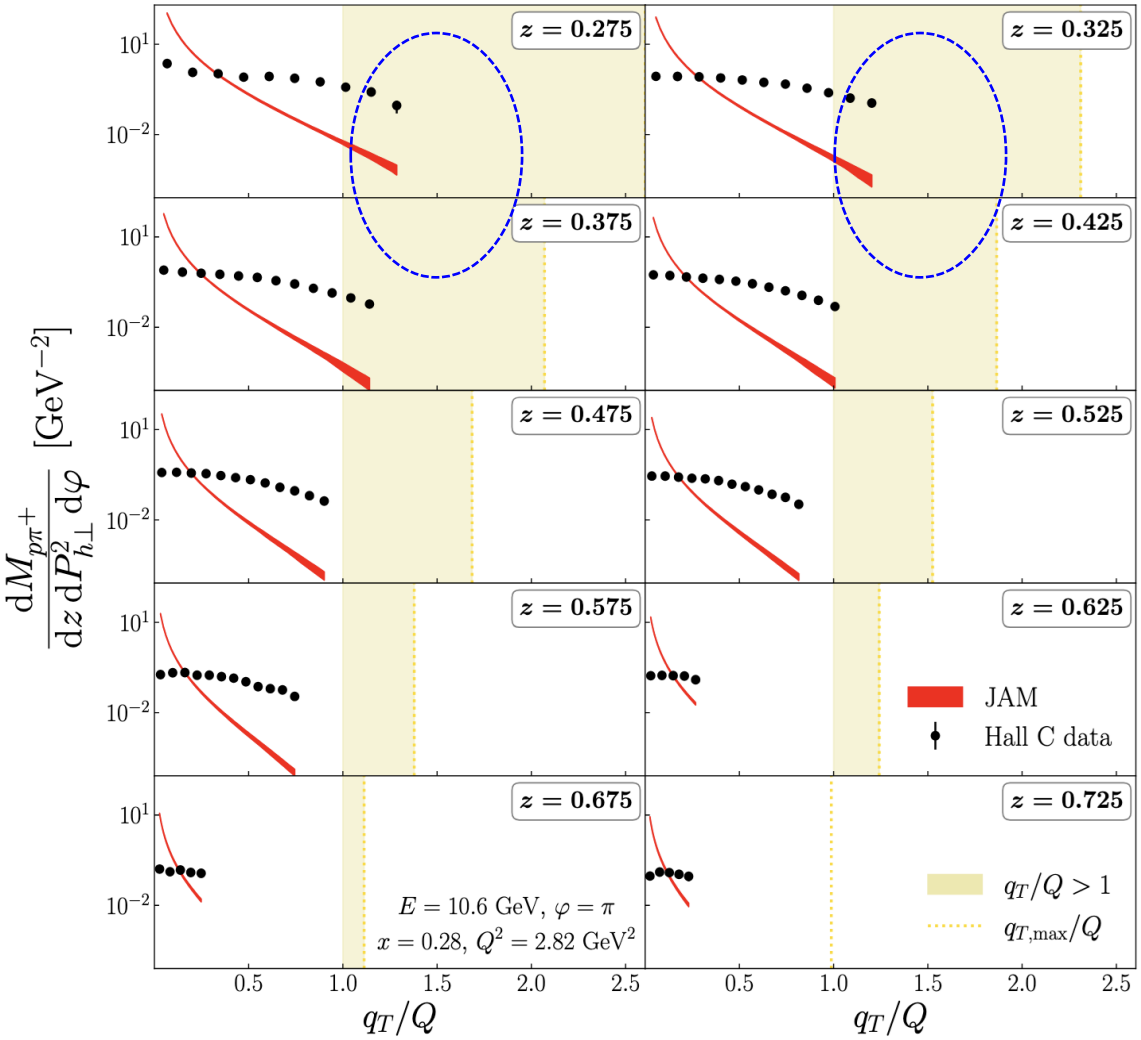


FIG. 6. Calculation analogous to Fig. 4 but for π^+ production measurements from Ref. [32].

$z_H > 0.2, q_T > Q$: collinear current fragmentation

Fixed-order pQCD calculations and SIDIS measurements (Jlab Hall-C)



$z_H > 0.2, q_T > Q$: collinear current fragmentation

Theoretical Studies

SIDIS: fixed-order theory–data tension

Gonzalez-Hernandez, Rogers, Sato & Wang
PRD 98, 114005 (2018)
Wang et al., PRD 99, 094029 (2019)

Drell–Yan: analogous high-qT tension

Bacchetta et al., PRD 100, 014018 (2019)

Power corrections near phase-space edges

Liu & Qiu, PRD 101, 014008 (2020)

QED radiation and reconstructed kinematics

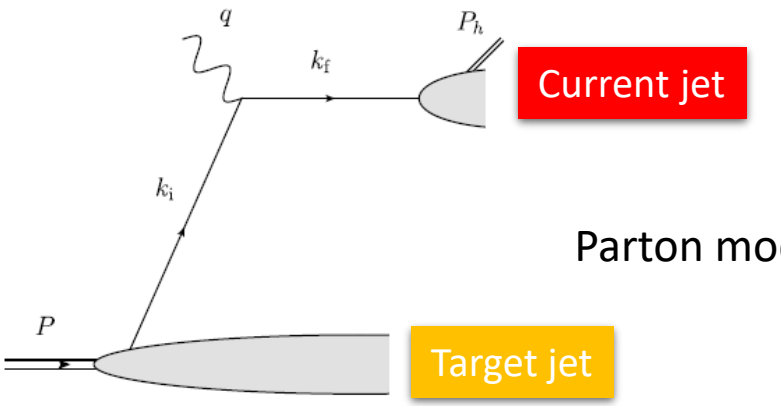
Liu, Melnitchouk, Qiu & Sato
PRD 104, 094033 (2021)
JHEP 11 (2021) 157

Matching the TMD and collinear regions

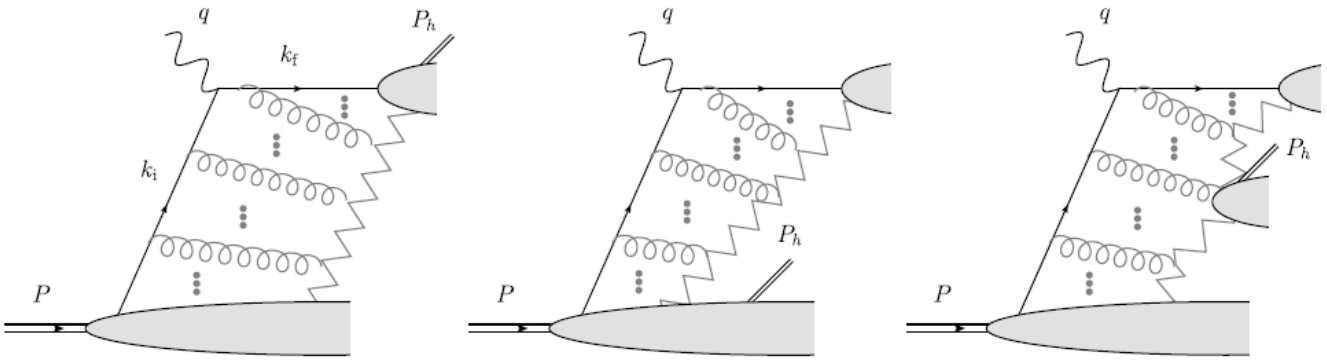
Boglione et al., JHEP 02 (2015) 095

SIDIS

$$l(l) + \text{Proton}(P) \rightarrow l'(l') + \text{Hadron}(P_H) + X$$



Parton model



(a) (b) (c)

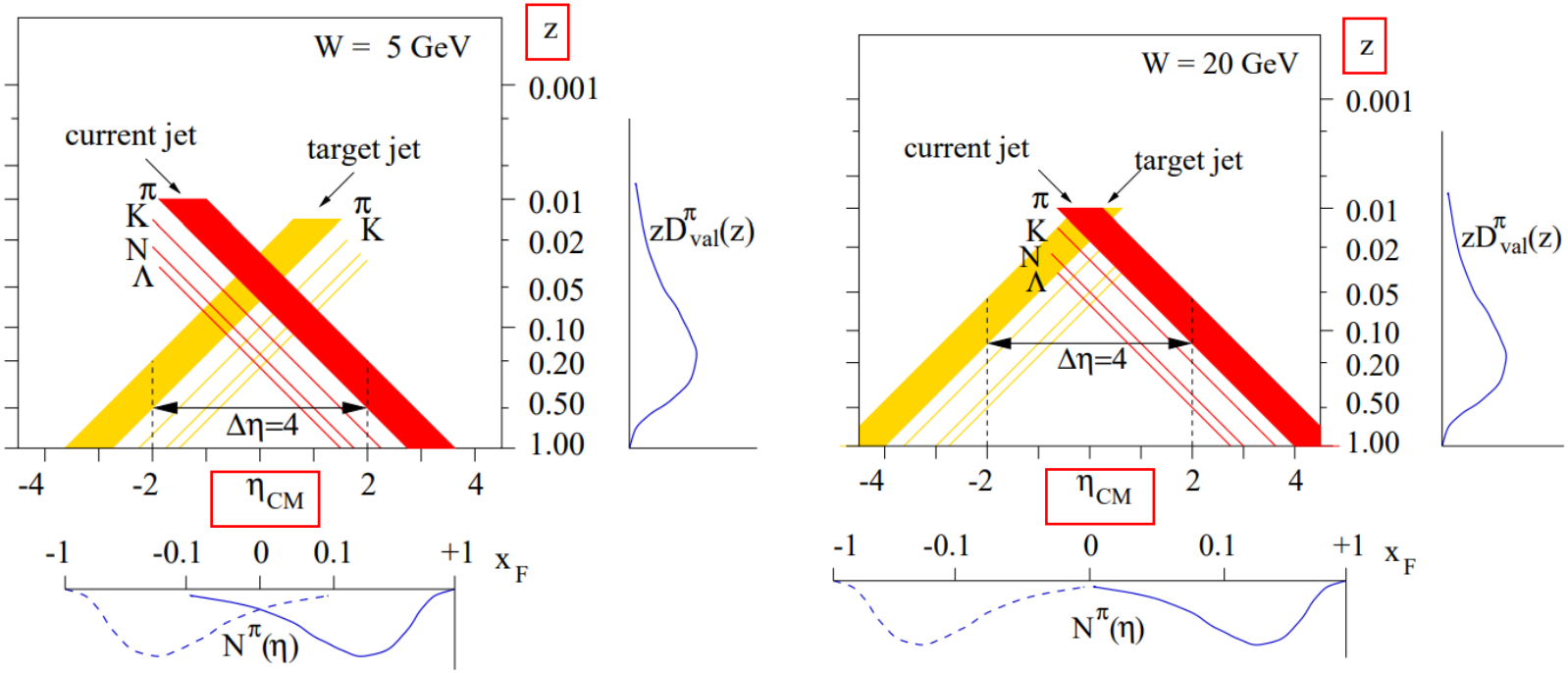
Current fragmentation | Target fragmentation | Central region

Separation of current fragmentation from target fragmentation

Berger criterion $\Delta\eta(z) > 2$

$$z_c(\eta) = \frac{P_h^-}{q^-} \qquad z_t(\eta) = \frac{P_h^+}{(1-x)P^+}$$

$$\eta = \frac{1}{2}\ln\left(\frac{P_h^-}{P_h^+}\right) = \ln\left(\frac{P_h^-\sqrt{2}}{M_{h\perp}}\right) = -\ln\left(\frac{P_h^+}{M_{h\perp}}\right)$$



The band reflects the influence of the transverse momentum.

https://arxiv.org/pdf/hep-ph/0010199

Hadron Rapidity (yh)

PLB 766(2017)245

$$z_{\rm h} = \frac{x_{\rm n} M_{h{\rm T}} M_p}{Q^2 - x_{\rm n}{}^2 M_p^2}\left(e^{y_p - y_{\rm h}} + e^{y_{\rm h} - y_p}\right)$$

$$= \frac{M_{h{\rm T}}}{Q^2 - x_{\rm n}{}^2 M_p^2}\left(Q\, e^{-y_{\rm h}} + \frac{x_{\rm n}{}^2 M_p^2}{Q} e^{y_{\rm h}}\right)$$

$$= \frac{M_{h{\rm T}}}{Q}\left(1 - x_{\rm n}{}^2 \frac{M_p^2}{Q^2}\right)^{-1}\left(e^{-y_{\rm h}} + x_{\rm n}{}^2 \frac{M_p^2}{Q^2} e^{y_{\rm h}}\right), \qquad (18)$$

where y_p is the proton rapidity

$$y_p = \ln\left(\frac{Q}{x_{\rm n} M_p}\right). \qquad (19)$$

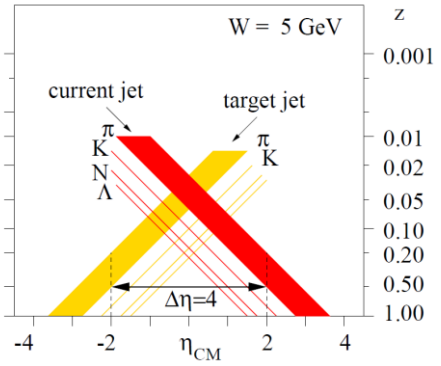
The inverse transformation is two-valued:

$$y_{\rm h}{}^{\pm} = \ln\left[\frac{Q z_{\rm h}\left(Q^2 - x_{\rm n}{}^2 M_p^2\right)}{2 x_{\rm n}{}^2 M_p^2 M_{h{\rm T}}} \pm \frac{Q}{x_{\rm n} M_p}\sqrt{\frac{z_{\rm h}{}^2\left(Q^2 - x_{\rm n}{}^2 M_p^2\right)^2}{4 x_{\rm n}{}^2 M_p^2 M_{h{\rm T}}^2} - 1}\right]. \qquad (20)$$

inappropriate. The value of $z_{\rm h}$ where $y_{\rm h} = 0$ is

$$z_{\rm h}(y_{\rm h} = 0) = \frac{M_{h{\rm T}}}{Q}\,\frac{1 + x_{\rm n}{}^2 M_p^2/Q^2}{1 - x_{\rm n}{}^2 M_p^2/Q^2}. \qquad (24)$$

At this value, the hadron is neither a left-mover nor a right-mover in the Breit frame.



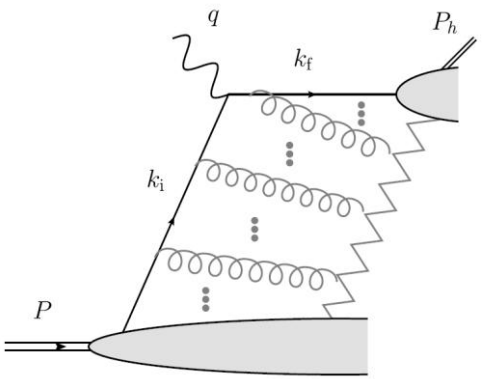
$$y_{\rm h}{}^{+} - y_p = y_p - y_{\rm h}{}^{-} \geq 0$$

y_h^+ : target fragmentation

y_h^- : current fragmentation

Quark Rapidity (yi, yf) in Breit Frame

PLB 766(2017)245



The canonical partonic power counting for the initial and final quark light-cone momenta in Fig. 1(a) is

$$k_i = \left(O(Q), O(m^2/Q), O(\mathbf{m})\right); \quad |k_i{}^2| = O(m^2), \tag{9}$$

$$k_f = \left(O(m^2/Q), O(Q), O(\mathbf{m})\right); \quad k_f{}^2 = O(m^2). \tag{10}$$

(Note that k_i is normally space-like.) For power counting purposes, m is to be understood as a combination of the small mass scales, $m \in \{\Lambda_{QCD}, M_p\}$. The actual quark light-cone momenta can be parametrized as

$$k_i = \left(\frac{M_{iT}}{\sqrt{2}} e^{y_i}, -\frac{M_{iT}}{\sqrt{2}} e^{-y_i}, \boldsymbol{k}_T\right), \tag{11}$$

$$k_f = \left(\frac{M_{fT}}{\sqrt{2}} e^{y_f}, \frac{M_{fT}}{\sqrt{2}} e^{-y_f}, \boldsymbol{k}_T\right), \tag{12}$$

$M_{(i/f)T}$: transverse masses of quarks, estimated from fits to data

$$M_{iT}^2 = M_{fT}^2 = 0.5 \pm 0.3 \text{ GeV}^2$$

Quark Rapidity (yi, yf) in Breit Frame

PLB 766(2017)245

The parton-model approximation sets $k_i{}^+ = -q^+$ and $k_f{}^- = q^-$. Hence the quark rapidities are approximately given by

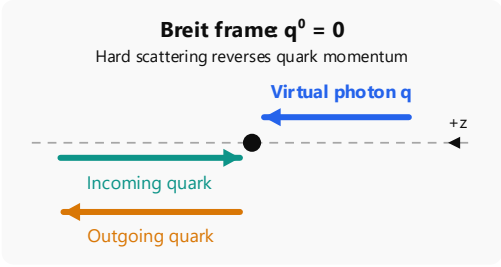
$$y_i = \ln \frac{Q}{M_{iT}}, \tag{13}$$

$$y_f = -\ln \frac{Q}{M_{fT}}, \tag{14}$$

which should be large (positive and negative, respectively) for factorization to hold true. Given a value for Q, the exact values of initial and final quark four-momenta could be determined from knowledge of M_{iT}^2, M_{fT}^2, and $\boldsymbol{k}_T$. In the limit that all of M_{iT}^2/Q^2, M_{fT}^2/Q^2, $\boldsymbol{k}_T$ go to zero, we have the basic parton-model formulas

$$k_i \approx \left(\frac{Q}{\sqrt{2}}, 0, \mathbf{0}_T\right), \tag{15}$$

$$k_f \approx \left(0, \frac{Q}{\sqrt{2}}, \mathbf{0}_T\right). \tag{16}$$



Collinearity (R)

PLB 766(2017)245

$$R(y_{\mathrm{h}}, z_{\mathrm{h}}, x_{\mathrm{bj}}, Q) \equiv \frac{P_h \cdot k_{\mathrm{f}}}{P_h \cdot k_{\mathrm{i}}}, \tag{27}$$

for which we identify

$$R(y_{\mathrm{h}}, z_{\mathrm{h}}, x_{\mathrm{bj}}, Q) \ll 1: \text{ collinear to outgoing quark}, \tag{28}$$

$$R(y_{\mathrm{h}}, z_{\mathrm{h}}, x_{\mathrm{bj}}, Q)^{-1} \ll 1: \text{ collinear to incoming quark}. \tag{29}$$

$R \leq 0.25$: current fragmentation

$R^{-1} < 0.25$: target fragmentation

PhT, yh, zh, R

$$P_{hT} = Q\sqrt{\frac{z_h^2(Q^2 - x_n^2 M_p^2)^2}{x_n^2 M_p^2 Q^2 \left(e^{y_p - y_h} + e^{y_h - y_p}\right)^2} - \frac{M_h^2}{Q^2}}$$

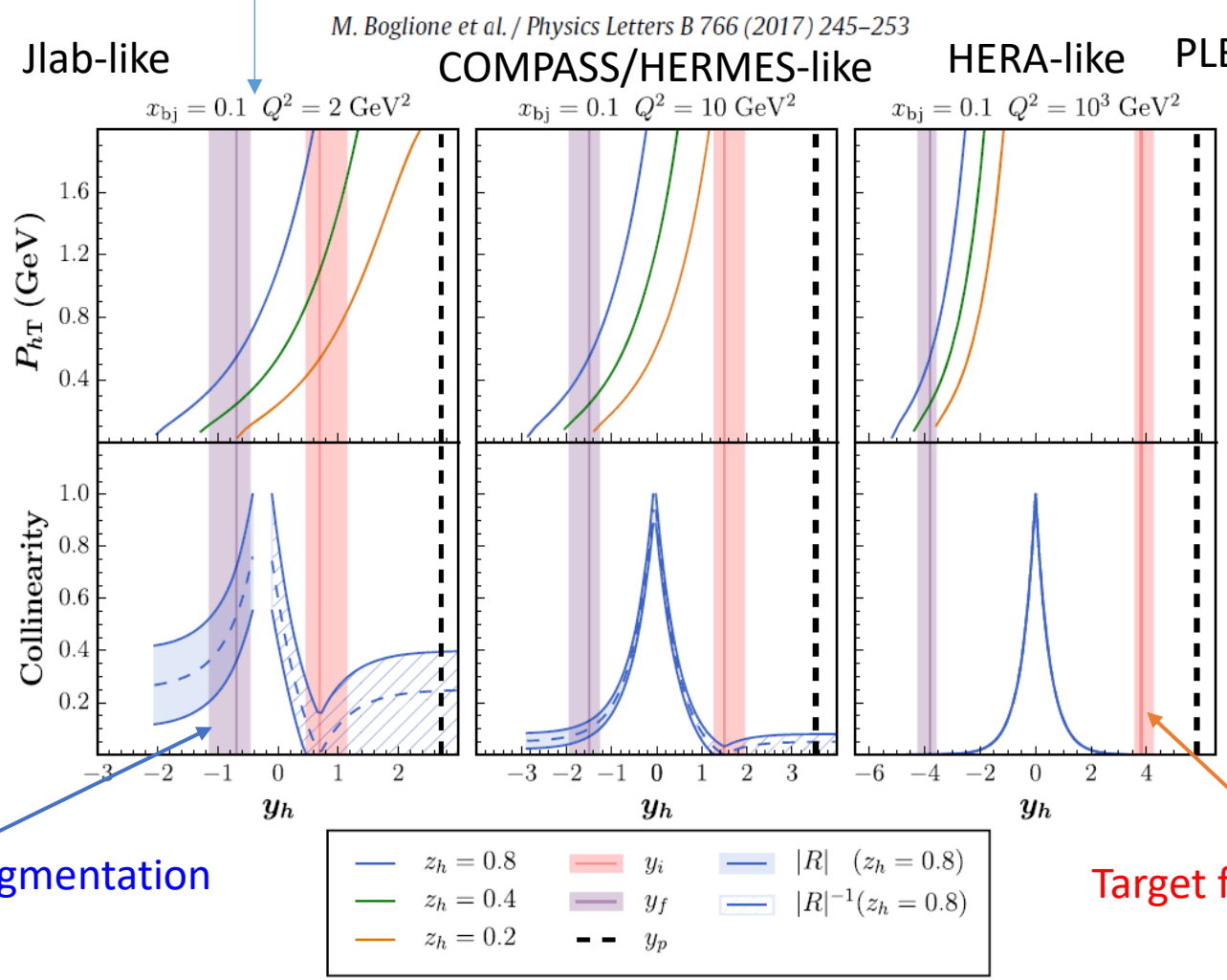
The small rapidity difference *yi* – *yf* also indicates that the applicability of the hard-scattering picture is quite marginal.

Jlab-like

COMPASS/HERMES-like

HERA-like

PLB 766(2017)245



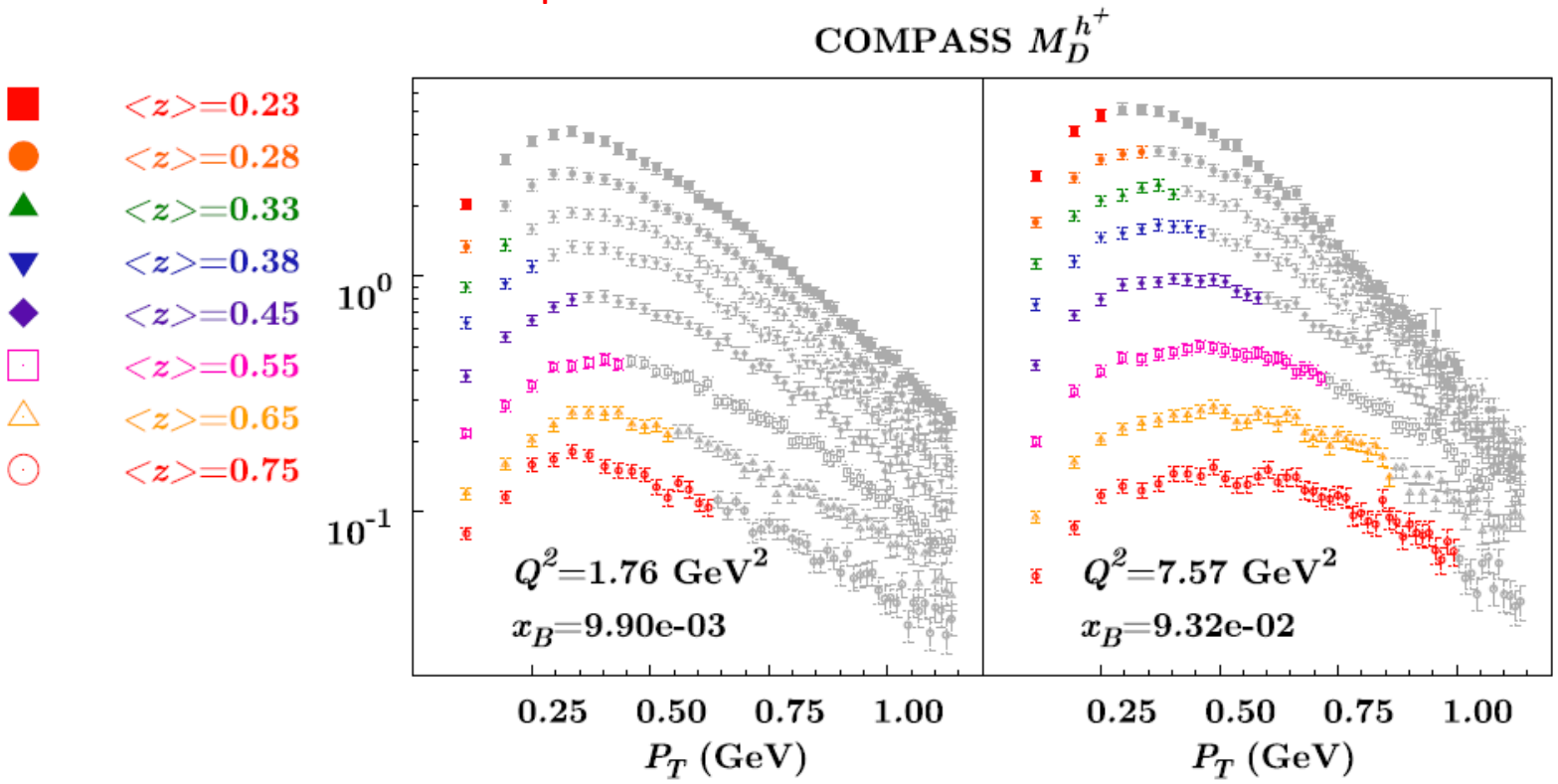
Current fragmentation

Target fragmentation

Safe/Ambiguous Regions

PLB 766(2017)245

Color points: R<0.25

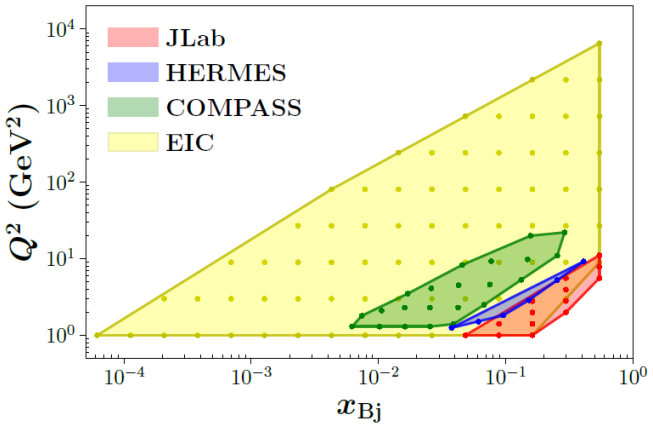


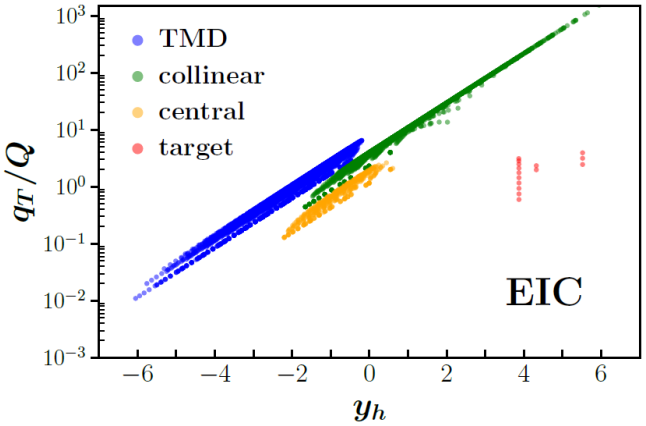
Grey points are likely to receive important contributions from non-current regions

SIDIS studies in EIC

- Wide phase space (Q2, xB)
- Large acceptance of particles (zh, PhT) or (yh, PhT)
- Good particle identification
- Measurements of SIDIS in various fragmentation regions and thus studies of the transition between them could be done systematically.

JHEP04(2022)084

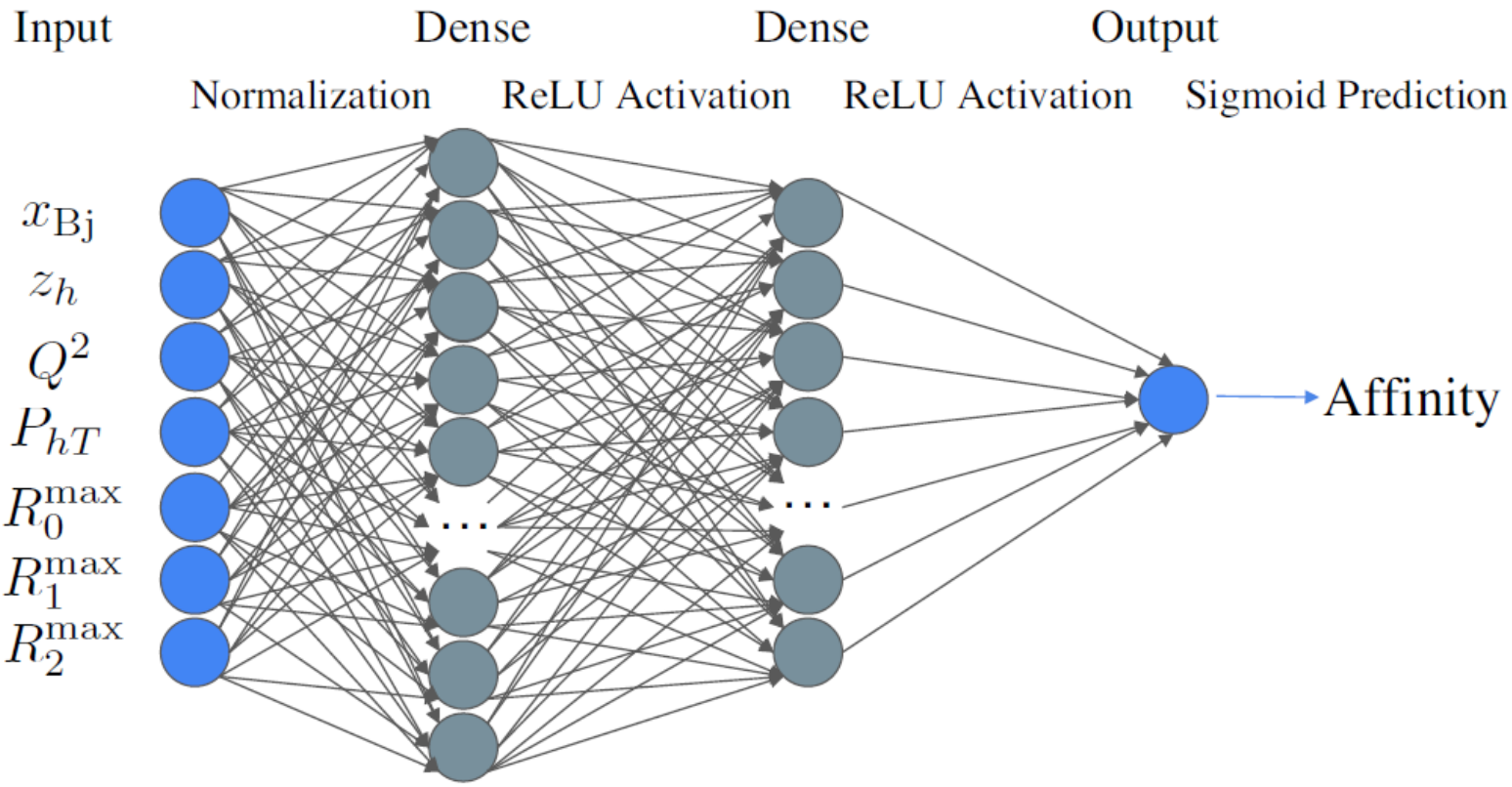




Affinity
(Global Event Estimator)

M. Boglione et al., *Affinity github repository*, https://github.com/QCDHUB/SIDIS-Affinity, (2022).

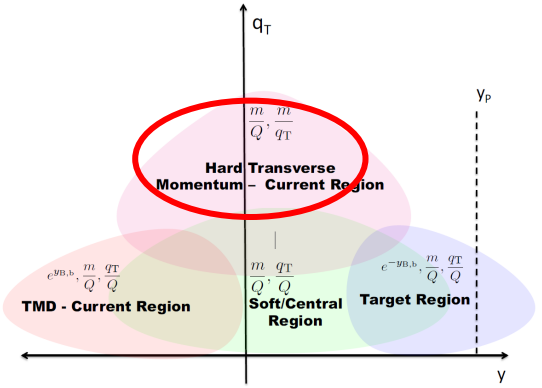
JHEP04(2022)084

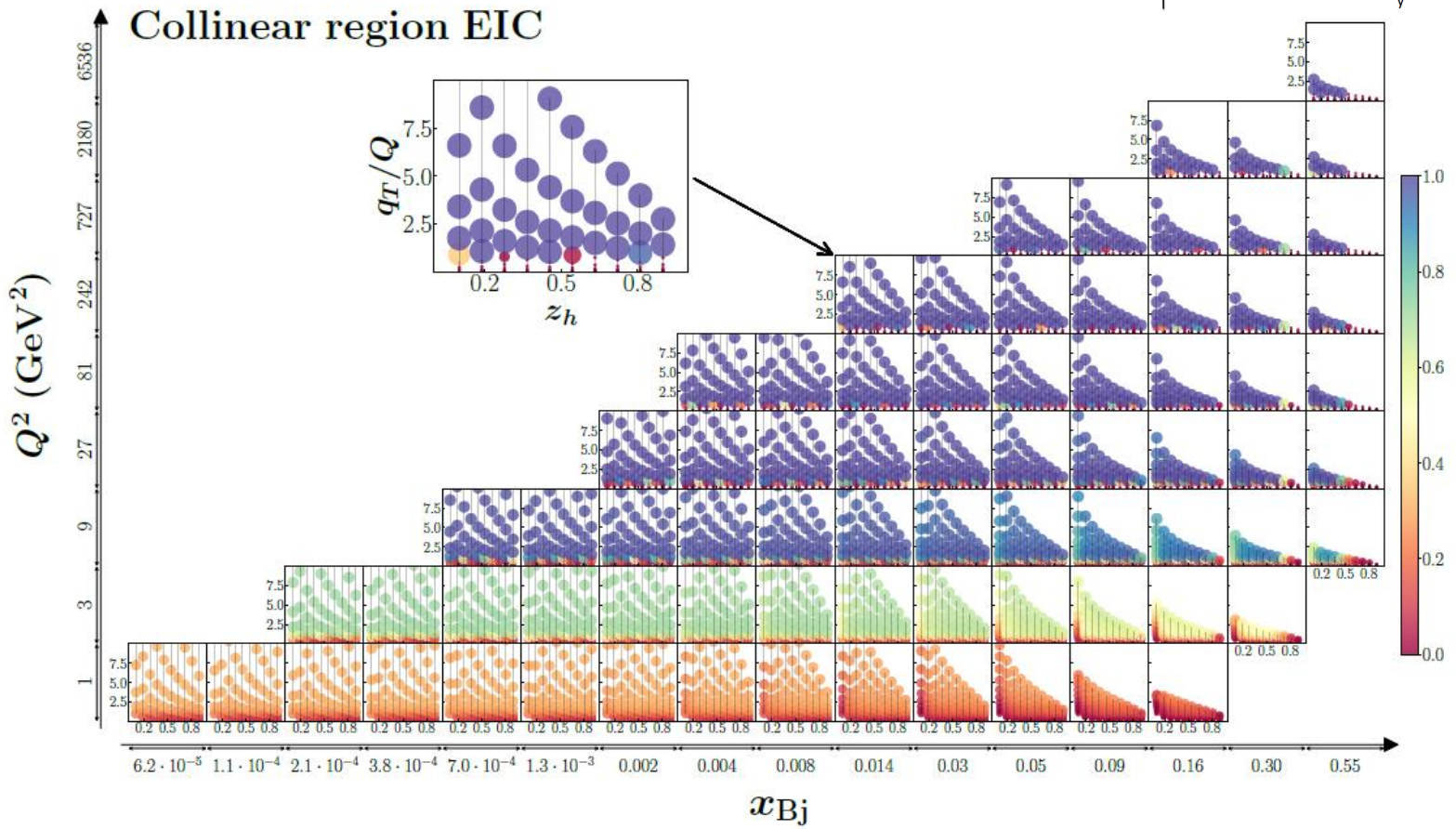


$$\mathcal{A}(x_{\rm Bj}, Q^2, z_h, P_{hT}|\text{region}) = \int \mathrm{d}\{R_i\}\ \ \Theta(\{R_i\}|\ \text{region})$$
$$\times \int \mathrm{d}^4k_i\, \mathrm{d}^4k_f\, \mathrm{d}^4\delta k_{\rm T}\ \mathcal{P}(\{R_i\}|x_{\rm Bj}, Q^2, z_h, P_{hT}; k_i, k_f, \delta k_T)\ \pi(k_i, k_f, \delta k_T),$$

from $\sqrt{s} = 20\,\text{GeV}$ to $140\,\text{GeV}$, we simulated semi-inclusive deep-inelastic π^+ production for 7400 bins in x_{Bj}, z_h, Q^2, and P_{hT}, as in the EIC Yellow Report EIC [42]. Figure 3

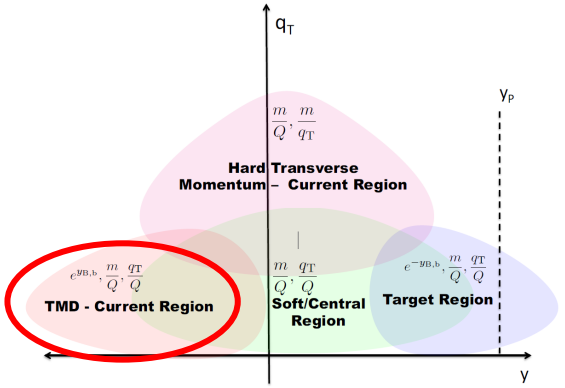
Affinity
(Global Event Estimator)

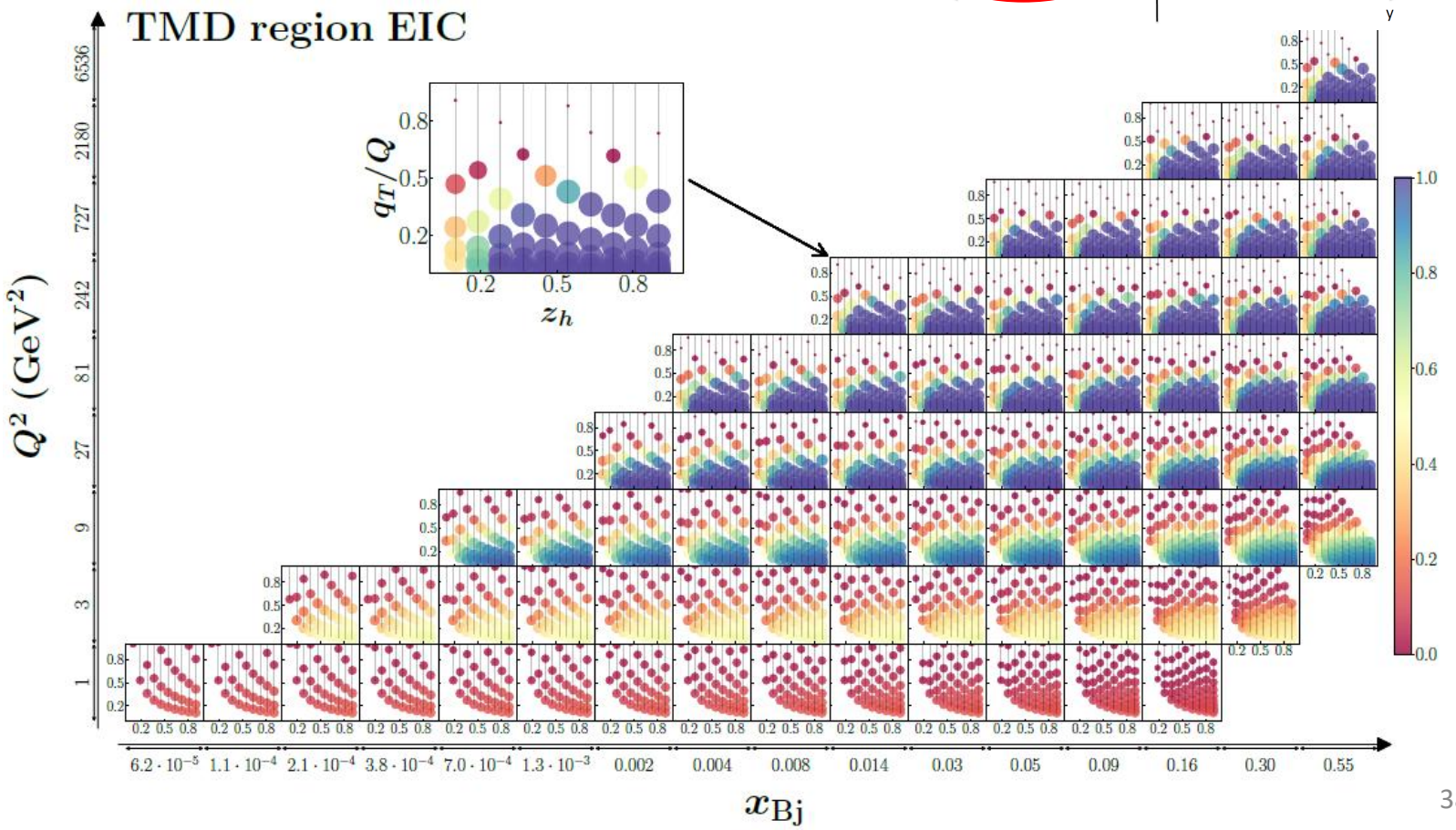




from $\sqrt{s} = 20\,\text{GeV}$ to $140\,\text{GeV}$, we simulated semi-inclusive deep-inelastic π^+ production for 7400 bins in x_{Bj}, z_h, Q^2, and P_{hT}, as in the EIC Yellow Report EIC [42]. Figure 3

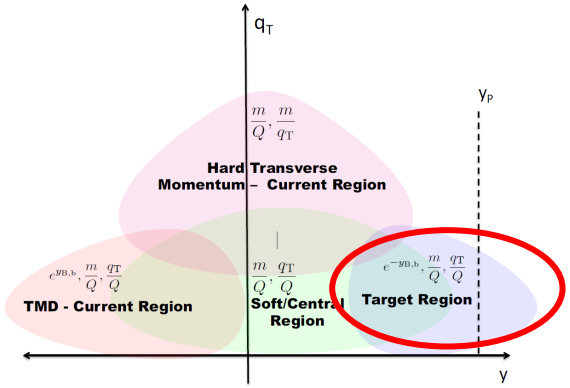
Affinity
(Global Event Estimator)

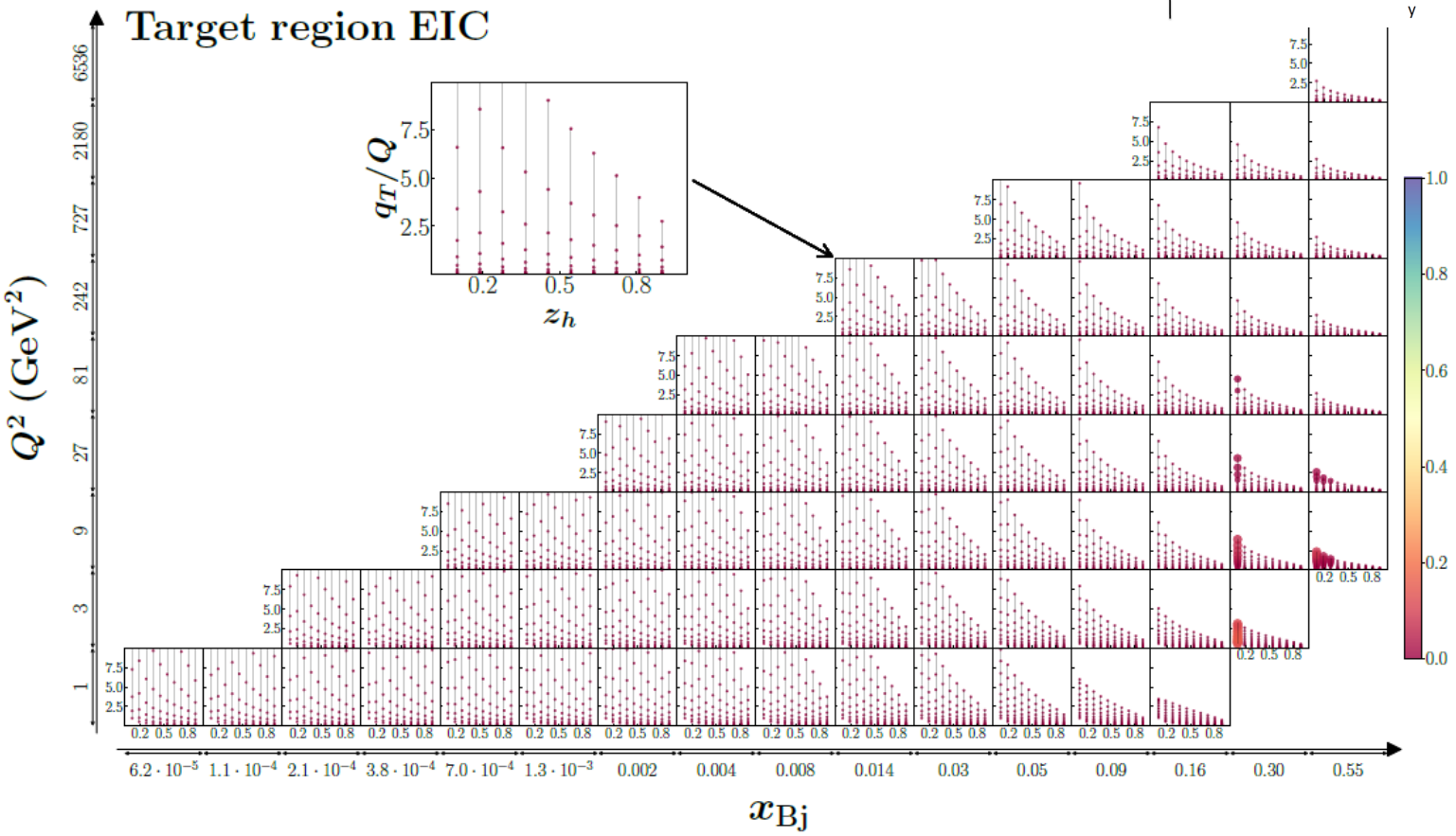




from $\sqrt{s} = 20\,\text{GeV}$ to $140\,\text{GeV}$, we simulated semi-inclusive deep-inelastic π^+ production for 7400 bins in x_{Bj}, z_h, Q^2, and P_{hT}, as in the EIC Yellow Report EIC [42]. Figure 3

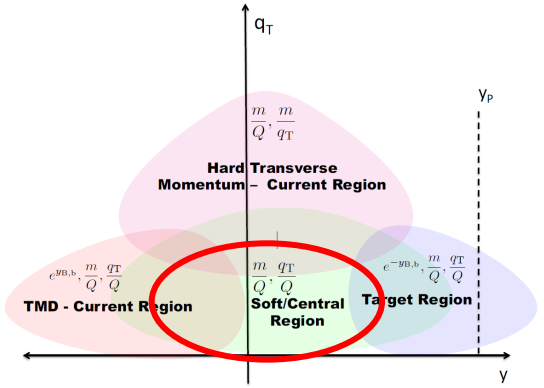
Affinity
(Global Event Estimator)

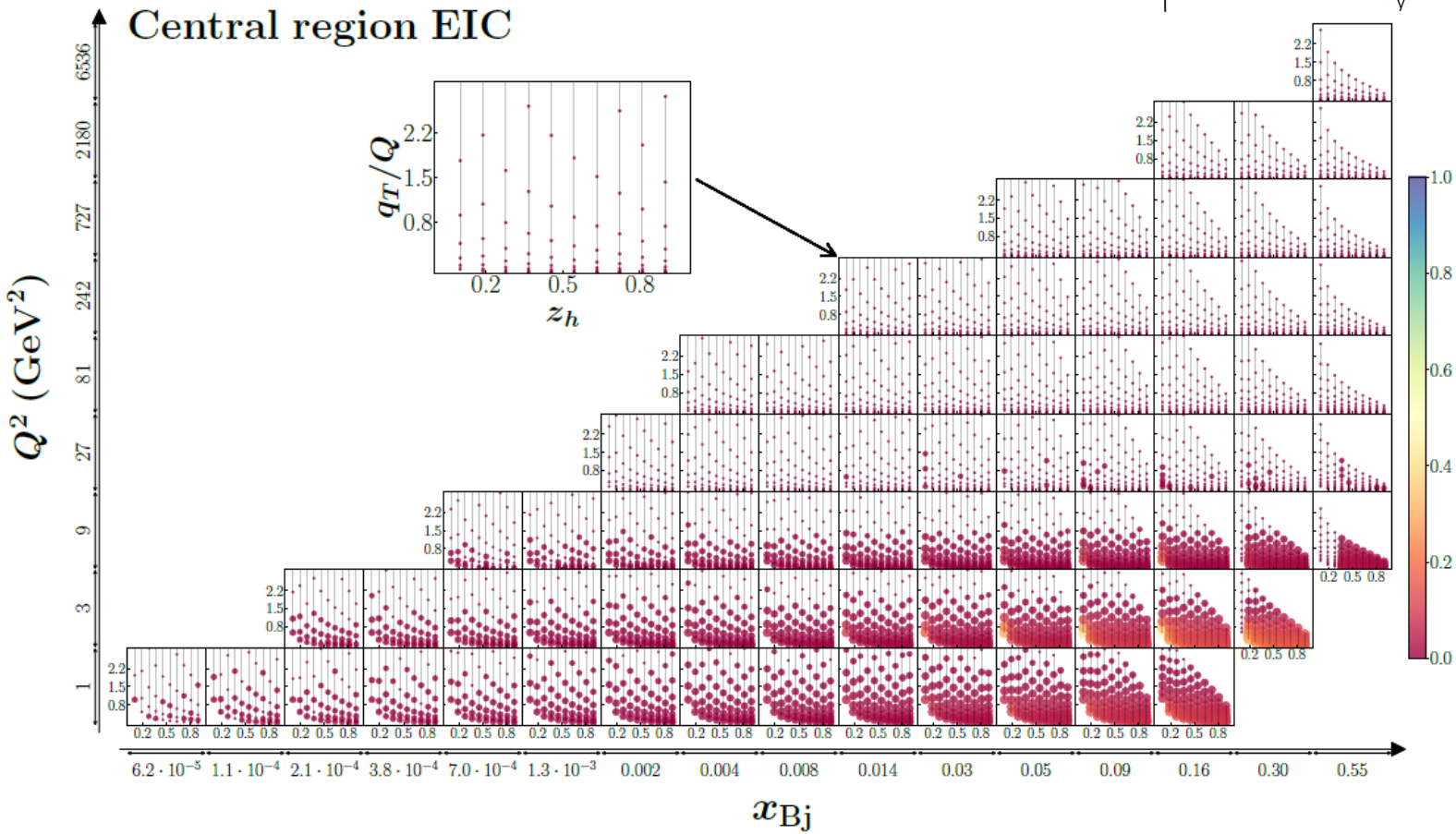




from $\sqrt{s} = 20\,\text{GeV}$ to $140\,\text{GeV}$, we simulated semi-inclusive deep-inelastic π^+ production for 7400 bins in x_{Bj}, z_h, Q^2, and P_{hT}, as in the EIC Yellow Report EIC [42]. Figure 3

Affinity
(Global Event Estimator)





Summary

- SIDIS is essential for studying the flavor dependence of PDFs and TMDs.
- The yields in the collinear regions are underestimated by the fixed-order pQCD calculations. Various propositions are given.
- Due to PhT, the conventional cut of zh>0.2 is not good enough to select the current fragmentation. There are proposed criteria of $\Delta\eta > 2$ or $\mathrm{R} > 0.25$.
- In EIC, we could carry out SIDIS measurements in wide kinetic spaces and might study the transition between them systematically.